

A handwritten signature in black ink, appearing to be 'AMR', is written over a horizontal line.

DRAFT DISCLAIMER

This contractor document was prepared for the U.S. Department of Energy (DOE), but has not undergone programmatic, policy, or publication review, and is provided for information only. The document provides preliminary information that may change based on new information or analysis, and is not intended for publication or wide distribution; it is a lower level contractor document that may or may not directly contribute to a published DOE report. Although this document has undergone technical reviews at the contractor organization, it has not undergone a DOE policy review. Therefore, the views and opinions of authors expressed do not necessarily state or reflect those of the DOE. However, in the interest of the rapid transfer of information, we are providing this document for your information, per your request.

T0115

OFFICE OF CIVILIAN RADIOACTIVE WASTE MANAGEMENT
ANALYSIS/MODEL COVER SHEET

1. QA: QA

Page: 1 of: 62

Complete Only Applicable Items


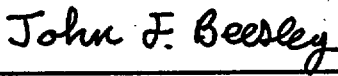


- | | |
|---|---|
| 2. <input checked="" type="checkbox"/> Analysis
<input type="checkbox"/> Performance Assessment
<input type="checkbox"/> Scientific | 3. <input type="checkbox"/> Model
<input type="checkbox"/> Conceptual Model Documentation
<input type="checkbox"/> Model Documentation
<input type="checkbox"/> Model Validation Documentation |
|---|---|

4. Title:
Effects of Fault Displacement on Emplacement Drifts

5. Document Identifier (including Rev. No. and Change No., if applicable):
ANL-EBS-GE-000004 REV 00

6. Total Attachments:
NONE

7. Attachment Numbers - No. of Pages in Each:
N/A

	Printed Name	Signature	Date
8. Originator	Fei Duan		2/3/2000
9. Checker	John F. Beesley		2/3/2000
10. Lead/Supervisor	Gerald R. Thiers		2/3/2000
11. Responsible Manager	Daniel G. McKenzie III		2/4/00

12. Remarks:

DF03

**OFFICE OF CIVILIAN RADIOACTIVE WASTE MANAGEMENT
ANALYSIS/MODEL REVISION RECORD**

1. Page: 2 of: 62

Complete Only Applicable Items

2. Analysis or Model Title:

Effects of Fault Displacement on Emplacement Drifts

3. Document Identifier (including Rev. No. and Change No., if applicable):

ANL-EBS-GE-000004 REV 00

4. Revision/Change No.

5. Description of Revision/Change

00

Initial Issue

CONTENTS

	Page
LIST OF ACRONYMS AND ABBREVIATIONS	7
1. PURPOSE.....	8
2. QUALITY ASSURANCE.....	9
3. COMPUTER SOFTWARE AND MODEL USAGE.....	10
4. INPUTS	11
4.1. DATA AND PARAMETERS.....	11
4.2. CRITERIA	11
4.3. CODES AND STANDARDS.....	12
5. ASSUMPTIONS.....	13
6. ANALYSIS.....	15
6.1. INTRODUCTION.....	15
6.1.1. Probabilistic Assessment of Fault Displacement.....	15
6.1.2. Design Methodology for Fault Displacement.....	18
6.1.3. Acceptance Criteria for Fault Displacement.....	18
6.2. LITERATURE SURVEY	19
6.3. APPROACH	19
6.3.1. General.....	20
6.3.2. Analytical Approximation for Normal and Reverse Faults	24
6.3.3. Analytical Approximation for Strike-Slip Faults.....	27
6.4. EVALUATION OF FAULT DISPLACEMENT EFFECTS.....	29
6.4.1. Normal and Reverse Faulting Scenarios.....	29
6.4.1.1 Verification of Routine Results.....	29
6.4.1.2 Induced Displacements and Stresses.....	32
6.4.2. Strike-Slip Faulting Scenario	50
6.5. DISCUSSION	52
6.5.1. Fault Displacement Effects on Drifts.....	52
6.5.2. Fault Displacement Effects on Drip Shields	53
6.5.3. Fault Displacement Effects on Waste Packages	57
7. CONCLUSIONS	58
8. REFERENCES	60
9. ATTACHMENTS.....	62

FIGURES

	Page
Figure 1. Normal Faulting Scenario	21
Figure 2. Reverse Faulting Scenario.....	22
Figure 3. Strike-Slip Faulting Scenario	23
Figure 4. Constant Displacement Discontinuity Concept Used for Fault Displacement Evaluation: (a) Mathematical Schematic for Closed-Form Solutions; (b) Application to the Emplacement Drift Vicinity.....	25
Figure 5. Simplified Strike-Slip Fault Diagram: (a) Prior to Faulting; (b) After Faulting.....	28
Figure 6. Induced Rock Movement at the Location of an Emplacement Drift vs. Fault Displacement with Half of the Fault Extent Equal to 100 m along the Dip	34
Figure 7. Induced Rock Movement at the Location of an Emplacement Drift vs. Fault Displacement with Half of the Fault Extent Equal to 400 m along the Dip	35
Figure 8. Induced Normal Stress at the Location of an Emplacement Drift vs. Fault Displacement: RMQ = 1, Distance between the Drift and Fault = 10 m.....	36
Figure 9. Induced Normal Stress at the Location of an Emplacement Drift vs. Fault Displacement: RMQ = 1, Distance between the Drift and Fault = 60 m.....	37
Figure 10. Induced Normal Stress at the Location of an Emplacement Drift vs. Fault Displacement: RMQ = 1, Distance between the Drift and Fault = 100 m.....	38
Figure 11. Induced Normal Stress at the Location of an Emplacement Drift vs. Fault Displacement: RMQ = 5, Distance between the Drift and Fault = 10 m.....	39
Figure 12. Induced Normal Stress at the Location of an Emplacement Drift vs. Fault Displacement: RMQ = 5, Distance between the Drift and Fault = 60 m.....	40
Figure 13. Induced Normal Stress at the Location of an Emplacement Drift vs. Fault Displacement: RMQ = 1, Distance between the Drift and Fault = 100 m.....	41
Figure 14. Induced Shear Stress at the Location of an Emplacement Drift vs. Fault Displacement: RMQ = 1, Distance between the Drift and Fault = 0 m.....	42
Figure 15. Induced Shear Stress at the Location of an Emplacement Drift vs. Fault Displacement: RMQ = 1, Distance between the Drift and Fault = 10 m.....	43
Figure 16. Induced Shear Stress at the Location of an Emplacement Drift vs. Fault Displacement: RMQ = 1, Distance between the Drift and Fault = 60 m.....	44
Figure 17. Induced Shear Stress at the Location of an Emplacement Drift vs. Fault Displacement: RMQ = 1, Distance between the Drift and Fault = 100 m.....	45
Figure 18. Induced Shear Stress at the Location of an Emplacement Drift vs. Fault Displacement: RMQ = 5, Distance between the Drift and Fault = 0 m.....	46
Figure 19. Induced Shear Stress at the Location of an Emplacement Drift vs. Fault Displacement: RMQ = 5, Distance between the Drift and Fault = 10 m.....	47
Figure 20. The Induced Shear Stress at the Location of an Emplacement Drift vs. Fault Displacement: RMQ = 5, Distance between the Drift and Fault = 60 m.....	48
Figure 21. Induced Shear Stress at the Location of an Emplacement Drift vs. Fault Displacement: RMQ = 5, Distance between the Drift and Fault = 100 m.....	49

Figure 22. Effect of a Strike-Slip Fault on Emplacement Drift Located below the Fault.....	51
Figure 23. A Schematic of Waste Package, Drip Shield and Backfill.	55
Figure 24. A Schematic Diagram for Estimating Fault Displacement Effects on Drip Shield: (a) Drift Excavation for Which Fault Displacement Effects Are Evaluated; (b) After Drip Shield Installation for Which Fault Displacement Effects Are to Be Estimated.....	56

TABLES

	Page
Table 1. Mean Fault Displacement at Principal Faults	17
Table 2. Mean Fault Displacement Away from Principal Faults.....	17
Table 3. Selected Spreadsheet Results for Comparing Hand Calculations	31
Table 4. Input Parameters for Spreadsheet Calculations	32
Table 5. Induced Shear Stress at the Emplacement Drift Location	53

LIST OF ACRONYMS AND ABBREVIATIONS

CRWMS	Civilian Radioactive Waste Management System
DBE	Design Basis Event
DOE	United States Department of Energy
ESF	Exploratory Studies Facility (Note: Currently, the name "Test Facilities" is used instead of the ESF. For traceability, the acronym "ESF" is still used in this analysis whenever it is cited from a reference that uses the word "ESF".)
MGR	Monitored Geologic Repository
M&O	Civilian Radioactive Waste Management System Management and Operating Contractor
NRC	Nuclear Regulatory Commission
OCRWM	Office of Civilian Radioactive Waste Management
Q	Qualified
QA	Quality Assurance
QAP	Quality Administrative Procedure(s)
QARD	Quality Assurance Requirements and Description for the Civilian Radioactive Waste Management Program
QL	Quality Level
RMQ	Rock Mass Quality
SSCs	Structures, Systems, and Components
SSFD	Seismic Source and Fault Displacement
TBD	To Be Determined

1. PURPOSE

The purpose of this analysis is to evaluate potential effects of fault displacement on emplacement drifts, including drip shields and waste packages emplaced in emplacement drifts. The output from this analysis not only provides data for the evaluation of long-term drift stability but also supports the Engineered Barrier System (EBS) process model report (PMR) and Disruptive Events Report currently under development. The primary scope of this analysis includes 1) examining fault displacement effects in terms of induced stresses and displacements in the rock mass surrounding an emplacement drift and 2) predicting fault displacement effects on the drip shield and waste package. The magnitude of the fault displacement analyzed in this analysis bounds the mean fault displacement corresponding to an annual frequency of exceedance of 10^{-5} adopted for the preclosure period of the repository and also supports the postclosure performance assessment.

This analysis is performed following the development plan prepared for analyzing effects of fault displacement on emplacement drifts (CRWMS M&O 1999a). The analysis will begin with the identification and preparation of requirements, criteria, and inputs. A literature survey on accommodating fault displacements encountered in underground structures such as buried oil and gas pipelines will be conducted. For a given fault displacement, the least favorable scenario in term of the spatial relation of a fault to an emplacement drift is chosen, and the analysis is then performed analytically. Based on the analysis results, conclusions are made regarding the effects and consequences of fault displacement on emplacement drifts. Specifically, the analysis will discuss loads which can be induced by fault displacement on emplacement drifts, drip shield and/or waste packages during the time period of postclosure.

2. QUALITY ASSURANCE

An activity evaluation (CRWMS M&O 1999b) in accordance with QAP-2-0, *Conduct of Activities*, has determined that the Quality Assurance (QA) program applies to this analysis because activities to be conducted in this analysis are subject to requirements described in the *Quality Assurance Requirements and Description* (QARD) document (DOE/OCRWM 1998a). The analysis involves emplacement drifts that are an item on the *Q-List* (DOE/OCRWM 1998b).

Classification of emplacement drifts to be discussed in this analysis has been documented in *Classification of the MGR Subsurface Facility System* (CRWMS M&O 1999c) in accordance with QAP-2-3, *Classification of Permanent Items*. Emplacement drifts are under the QL-1 classification, subject to TBV-458 and TBV-460. Quality designator QL-1 is for those structures, systems and components (SSCs) whose failure could directly result in a condition adversely affecting public safety.

Although the ground control system is an integral part of emplacement drifts, no ground support for emplacement drifts can provide resistance to fault displacement if a fault intersects an emplacement drift. In addition, a conservative perception is that ground support systems will lose their function during postclosure. Therefore, the ground control system is not considered as a major item for this analysis. It is worth pointing out that the ground control system for emplacement drifts has been classified as QL-2 per *Classification of the MGR Ground Control System* (CRWMS M&O 1999d). Quality designator QL-2 is for those SSCs whose failure or malfunction could indirectly result in a condition adversely affecting public safety, or whose direct failure would result in consequences in excess of normal operational limits.

3. COMPUTER SOFTWARE AND MODEL USAGE

A software routine was developed within *Microsoft Excel 97* to perform algebraic computations based on closed-form solutions and to illustrate the results graphically. The routine documentation requirements of AP-SI.1Q, *Software Management*, Subsection 5.1 are addressed in Section 6.4.1.1 where the routine results are verified through hand calculations and visual inspection. No other engineering software was used in this analysis. In addition, the analysis did not involve models which represent a process, system or phenomenon.

4. INPUTS

Inputs to this analysis consist of 1) data and parameters required for computation, 2) criteria required to be met, and 3) codes and standards used.

4.1. DATA AND PARAMETERS

Although there are five rock mass quality (RMQ) categories established, with category 1 (i.e., RMQ = 1) representing the rock mass in heavily jointed condition and category 5 (i.e., RMQ = 5) in nearly intact condition, only category-1 and -5 rock mass properties will be used for this analysis. The rock mass modulus of elasticity (E) for the TSw2 unit is 8.98 GPa for RMQ = 1 and 24.71 GPa for RMQ = 5 (CRWMS M&O 1999e, p. 20) while the mean Poisson's ratio (ν) value for the TSw2 unit is 0.21 (CRWMS M&O 1999e, p. 21). The shear modulus (G) for each category is given by $G = E/[2(1+\nu)]$.

The range of fault displacement values considered in this analysis is based on those given in the report entitled *Probabilistic Seismic Hazard Analyses for Fault Displacement and Vibratory Ground Motion at Yucca Mountain, Nevada* (CRWMS M&O 1998d). The mean fault displacement for the classes of faults and fractures present in the repository block ranges from less than 0.1 cm to 32 cm corresponding to an annual frequency of exceedance of 10^{-5} (CRWMS M&O 1998d, Table ES-3). For annual exceedance probabilities below 10^{-5} , the mean fault displacements are graphically shown in the report (CRWMS M&O 1998d, Figures 8-2 through 8-14). These mean fault displacement values are calculated by probabilistic hazard analyses at nine demonstration sites in the repository vicinity. A brief description of these nine demonstration points, which represent the range of faulting conditions present in the repository block is given in CRWMS M&O 1998d, pp. 4-54 to 4-56. The fault displacement range from 0.1 to 100 cm is adopted to bound the mean values given by probabilistic seismic hazard analyses (CRWMS M&O 1998d, Table ES-3).

4.2. CRITERIA

Applicable criteria for performing this analysis are cited in the following. Section 6 of this analysis shows discussions on how these criteria are met.

- 4.2.1 A minimum standoff distance of 60 m shall be accommodated from the closest edge of the repository openings to the main trace of Type-I fault zone. (CRWMS M&O 1998a, Section 1.2.1.7). This standoff distance is TBV, but it does not need confirmation for this analysis, and will not be tracked.
- 4.2.2 A 15 m standoff between waste packages and Type-I faults and a 5 m standoff between waste packages and splays associated with Type-I faults shall be accommodated by emplacement drifts. (CRWMS M&O 1998a, Section 1.2.1.8)
- 4.2.3 Fault displacements (CRWMS M&O 1998b, Section 1.2.2.1.3) will be considered in the repository design.

4.3. CODES AND STANDARDS

There are no industry codes or standards directly applicable to this analysis.

5. ASSUMPTIONS

A number of assumptions are made in order to perform this analysis. Some of the assumptions are to facilitate a bounding analysis scenario while other assumptions are made to idealize or simplify the analysis.

- 5.1 The displacement along the fault is assumed to be constant. This assumption is based on the reasoning that a fault displacement is the result of sudden slip initiated at one location along the fault. Such a slip propagates through the entire rupture area so rapidly that the hanging and foot walls move relatively to each other almost like two rigid plates (i.e., any dragging effect or deformation in the fault zone is negligible), suggesting the constant fault displacement along the fault to be a reasonably conservative assumption. This assumption does not need to be confirmed and TBV tracking is not required. (Sections 6.3.2 and 6.3.3)
- 5.2 For a normal fault, only two special fault orientations are evaluated for fault displacement effect: one is parallel to the drift axis and the other is perpendicular to the drift axis. The former will make the most impact on emplacement drifts while the latter will have the least impact on emplacement drifts. Since effects from faults orientated in other directions with respect to the drift axis will be bounded by the two special orientations, this assumption does not need to be confirmed and TBV tracking is not required. (Section 6.3.2)
- 5.3 For a strike-slip fault, evaluation is only performed for the fault orientation that is parallel to the drift alignment. Furthermore, the analysis assumes that emplacement drifts lie directly underneath the strike-slip fault. This assumption allows for considering the maximum effect of fault displacement and is a conservative assumption. This assumption does not need to be confirmed and TBV tracking is not required. (Section 6.3.3)
- 5.4 All types of faults discussed in this analysis are assumed to be planar along the fault. This assumption is necessary to the computation of induced stresses and displacements presented in Section 6. This assumption is based on the general literature description on faults. This assumption does not need to be confirmed and TBV tracking is not required. (Sections 6.3.2 and 6.3.3)
- 5.5 Faults are considered to be sharp, meaning that the fault width is virtually zero. This assumption is needed to simplify the computation and is considered to be conservative for estimating fault displacement effects because a wider fault zone absorbs more energy which otherwise affects the rock. This assumption does not need to be confirmed and TBV tracking is not required. (Sections 6.3.2 and 6.3.3)
- 5.6 The fault length is assumed to be infinite, so that a two-dimensional simplification is valid. This assumption is considered to be conservative for evaluating fault displacement effects. This assumption does not need to be confirmed and TBV tracking is not required. (Sections 6.3.2 and 6.3.3)

- 5.7 The vertical in situ stress is gravitational while the horizontal in situ stress ranges from 0.3 to 1.0 times the vertical one (CRWMS M&O 1998c, p. 28). A bounding value for the vertical in situ stress at the repository host horizon is 10 MPa (CRWMS M&O 1998c, p. 28). Since all in situ stress components considered here correspond to the bounding value, no TBV tracking is needed, and for the purpose of this document the stresses do not require confirmation. (Section 6.4.2)
- 5.8 The length of a fault where fault displacement occurs is assumed to have the following range: 100, 200, 300, and 400 m. These lengths are considered not only to be sufficiently large relative to the drift diameter but also to allow for examining the trend of fault eruption length. This assumption does not need to be confirmed and TBV tracking is not required. (Sections 6.4.1 and 6.4.2)
- 5.9 The normal distance from an emplacement drift location to the fault is assumed to range from 0 to 100 m. This range goes beyond the minimum fault offset criterion and is considered to be adequate for this analysis. This assumption does not need to be confirmed and TBV tracking is not required. (Sections 6.4.1 and 6.4.2)
- 5.10 The depth of faulting is assumed to be greater than the length of a fault where fault displacement occurs (Assumption 5.8). This assumption is needed to validate the closed-form solutions present in Section 6.3.2 and is considered to be reasonable in light of the depth for the emplacement drift horizon (i.e., > 300 m). This assumption does not need to be confirmed and TBV tracking is not required. (Section 6.3.2)
- 5.11 For a normal or reverse fault, the angle of dip is not considered in computing fault-induced stresses or displacements which are referred to a local coordinate system (x-y-z), i.e., the x-axis is parallel to the fault while the y-axis is perpendicular to the fault. The angle of dip is only needed for superimposing the induced stresses and displacements onto those existing prior to faulting. Such a superimposition is not carried out in this analysis. This assumption does not need to be confirmed and TBV tracking is not required. (Section 6.3.2)

6. ANALYSIS

6.1. INTRODUCTION

This section provides a summary of work that has been done towards evaluating and accommodating fault displacement, including probabilistic assessment of fault displacement hazard, design methodology for fault displacement, and discussion on acceptance criteria for fault displacement in engineering design for emplacement drifts.

6.1.1. Probabilistic Assessment of Fault Displacement

Fault displacement hazards in the Yucca Mountain vicinity have been characterized and documented in a recent report entitled *Probabilistic Seismic Hazard Analyses for Fault Displacement and Vibratory Ground Motion at Yucca Mountain, Nevada* (CRWMS M&O 1998d). The report summarizes seismic source and fault displacement evaluations performed by six expert teams and facilitated by a Seismic Source and Fault Displacement (SSFD) Facilitation Team. In the report, nine demonstration points were selected for fault displacement hazard assessment. These points represent the expected range of faulting conditions in the controlled area in terms of the types of features that may be encountered, including 1) block-bounding faults with greater than 50 m of cumulative offset that may be seismogenic, 2) mapped intrablock faults with north-south and northwest-southeast strikes showing a few to tens of meters of cumulative displacement, and 3) features observed within the Test Facilities (TF) at the Yucca Mountain that are likely to be encountered within the proposed repository block. As is mentioned in Section 4.1 of this analysis, these selected points are described in CRWMS M&O 1998d, pp. 4-54 to 4-55, as follows:

Point 1. A location on the Bow Ridge fault where it crosses the ESF. The Bow Ridge fault is a block-bounding fault that has been characterized by the SSFD expert teams as being a potentially seismogenic fault and /or to be part of a seismogenic fault system.

Point 2. A location on the block-bounding Solitario Canyon fault, which has been characterized by the expert teams as one of the longer seismogenic faults within the Yucca Mountain site vicinity.

Point 3. A location on the Drill Hole Wash fault where it crosses the ESF, which is one of the longer northwest-striking faults within the Yucca Mountain site vicinity.

Point 4. A location on the Ghost Dance fault, which is one of the longer north-south intrablock faults within the controlled area.

Point 5. A location on the Sundance fault within the proposed repository footprint west of the TF. The Sundance fault is an intermediate size, northwest-trending intrablock fault.

Point 6. A location on a small fault mapped in bedrock on the west side of Dune Wash. This point represents a location on one of the many small north-south-striking intrablock faults that have been mapped at the surface of Yucca Mountain.

Point 7. A location approximately 100 m east of Solitario Canyon at the edge of the proposed repository footprint. Any one of four hypothetical conditions were assumed to exist at this location that are representative of features encountered within the ESF that are not directly correlated with specific features observed at the surface.

- (a) A small fault having 2 m of cumulative displacement
- (b) A shear having 10 cm of cumulative displacement
- (c) A fracture having no measurable displacement
- (d) Intact rock

Point 8. A location within the proposed repository footprint midway between the Solitario Canyon and Ghost Dance faults. The same four hypothetical conditions described at Point 7 were assumed to exist.

Point 9. A location in Midway Valley east of the Bow Ridge fault on an observed fracture having no measurable displacement in Quaternary alluvium.

A probabilistic fault displacement hazard analysis was made at each of these nine demonstration sites. The mean displacement hazard results corresponding to the two annual exceedance probabilities, 10^{-4} and 10^{-5} , are shown in Tables 1 and 2 (CRWMS M&O 1998d, Table ES-3). Table 1 tabulates the mean fault displacement at principal faults that consist of points 1 and 2. Table 2 shows the mean fault displacement away from principal faults.

It must be pointed out that the two annual exceedance probabilities, 10^{-4} and 10^{-5} , are considered for the preclosure period of the repository. Should a lower annual exceedance probability be considered, the corresponding mean fault displacement value would increase (CRWMS M&O 1998d, Figures 8-4 through 8-14). Since the mean postclosure fault displacement values are not readily available, their effects are not addressed in a direct manner. Some relevant discussions are provided in Section 6.5.

Table 1. Mean Fault Displacement at Principal Faults

Location	Mean Displacement (cm) Annual Frequency of Exceedance		Source
	10^{-4}	10^{-5}	
1. Bow Ridge Fault	<0.1	7.8	Listed in Section 4.1
2. Solitario Canyon Fault	<0.1	32	

Table 2. Mean Fault Displacement Away from Principal Faults

Location	Mean Displacement (cm) Annual Frequency of Exceedance		Source
	10^{-4}	10^{-5}	
3. Drill Hole Wash Fault	<0.1	<0.1	Listed in Section 4.1
4. Ghost Dance Fault	<0.1	<0.1	
5. Sundance Fault	<0.1	<0.1	
6. Unnamed fault west of Dune Wash	<0.1	<0.1	
7a. A hypothetical small fault with 2 m of offset, located 100 m east of Solitario Canyon Fault	<0.1	<0.1	
7b. A hypothetical shear with 10 cm of offset, located 100 m east of Solitario Canyon Fault	<0.1	<0.1	
7c. A hypothetical fracture, located 100 m east of Solitario Canyon Fault	<0.1	<0.1	
8a. Intact rock, located 100 m east of Solitario Canyon Fault	<0.1	<0.1	
8b. A hypothetical small fault with 2 m of offset, located between the Solitario Canyon Fault and the Ghost Dance Fault	<0.1	<0.1	
8c. A hypothetical shear with 10 cm of offset, located between the Solitario Canyon Fault and the Ghost Dance Fault	<0.1	<0.1	
8d. A hypothetical fracture, located between the Solitario Canyon Fault and the Ghost Dance Fault	<0.1	<0.1	
9. Intact rock, located between the Solitario Canyon Fault and the Ghost Dance Fault	<0.1	<0.1	

6.1.2. Design Methodology for Fault Displacement

A topical report on *Preclosure Seismic Design Methodology for a Geologic Repository at Yucca Mountain* (DOE/OCRWM 1997) describes the methods to be used to meet the pertinent preclosure safety performance objectives with respect to fault displacements. Three approaches are available, of which the primary method will be fault avoidance to the extent reasonably achievable by layout of the repository and placement of the drifts. Some guidance for determining fault setback can be obtained from engineering evaluations of expected responses of drifts to fault displacement.

In establishing fault displacement design criteria, the NRC guidance provided in NUREG-1494, *Staff Technical Position on Consideration of Fault Displacement Hazards in Geologic Repository Design* (NRC 1994) recommends that Type I faults within the geologic repository operations area be avoided when reasonably achievable. Type I faults are defined in NUREG-1451, *Staff Technical Position on Investigations to Identify Fault Displacement Hazards and Seismic Hazards at a Geologic Repository* (NRC 1992), as faults or fault zones that are subject to displacement and are of sufficient length and location such that they may affect repository design or performance. NUREG-1494 recommends fault avoidance but explicitly recognizes that fault avoidance may not be possible for all repository structures, especially drifts. When faults cannot be avoided, the potential for fault displacement will be accommodated through design or by repair and rehabilitation actions.

6.1.3. Acceptance Criteria for Fault Displacement

Acceptance criteria for fault displacement represent the level of tolerance to fault displacement-induced loads and damage when fault avoidance cannot be achieved during the emplacement drift design process. Such criteria have not been available at the time of this analysis. It is beyond the scope of this analysis to develop a set of acceptance criteria. Instead, the following rationale are discussed, which not only bring fault displacement effects to design perspective but also aid in reaching tentative conclusions of this analysis.

Hypothetically, given a circular emplacement drift intersected by a fault, any considerable fault displacement can render the drift no longer circular, possibly impeding the operational envelope requirement and transferring some loads to drip shields, if installed, or waste packages through backfill. As the drift wall is sheared and offset by the fault, the ground support system is loaded and may deform such that the elastic limit of the system is exceeded, and rock falls may follow. Therefore, acceptance criteria are required for emplacement drift clearance, ground support systems, and waste packages/drip shields.

In general, once the design basis fault displacements are determined, the resulting loads (or stresses) and deformations (or strains) in a ground control system can be calculated using numerical methods that will consider lining and rock mass stiffnesses, and lining configuration. Unlike vibratory ground motion loads, however, fault displacement loads are generally localized and often cause inelastic response (unless the structure and the ground medium are very flexible, in which case the lining can undergo large deformation and stay within elastic limits). For this reason, strain-based acceptance criteria are preferable to stress-based ones in establishing the design adequacy of structures subjected to fault displacement loads (DOE/OCRWM 1997).

Actions that can be taken to ensure safe performance of drifts at crossings of Type I faults consist of excavation of an oversized section of an emplacement drift through the fault zone and use of flexible support systems, e.g., by incorporation of a flexible coupling (such as a yielding or sliding sleeve) in the ground support system. For waste packages and drip shields, if installed, strain-based acceptance criteria can be established to dictate the maximum level of tolerance of fault displacement-induced strains so that adequate design measure can be taken to meet the criteria.

6.2. LITERATURE SURVEY

Technical literature that is relevant to the fault displacement evaluation presented in this analysis is limited. Nevertheless, design consideration for both tunnels through faults and fault crossing for buried pipelines is worth mentioning. A number of examples of tunnel design and performance through faults are discussed as case histories in a topical report (DOE/OCRWM 1997). Fault displacement in most of the case histories is due to rupture during an earthquake, although a few cases are given where fault creep is the primary source of movement. Review of the tunnel design case histories has indicated that there were no design provisions to accommodate fault displacement, particularly for the tunnels constructed prior to the 1950s. When fault displacement damage to tunnels occurred, the common approach was to make necessary repairs. More recent approaches to tunnel fault displacement design include evaluating the necessity for accommodating fault displacement and providing the flexibility to tolerate tunnel deformation associated with fault displacement without undue disruption of the tunnel function. Clearly, those tunnel design case histories provide little insight into fault displacement effects on backfill and waste package emplaced in drifts.

Studies of fault displacement effects on buried oil pipeline systems have been reported by many researchers such as Kennedy et al. 1977, Duncan and LeFebvre 1973, and Kennedy et. al. 1979. Both analytical approximations and numerical simulations have been used to determine fault displacement effects. Recognizing that oil pipelines are generally buried shallow in soil and that any differential soil movement will load pipelines immediately, approaches used for analyzing fault crossings for pipelines do not shed much light on fault displacement problems for emplacement drifts. Emplacement drifts are located deep in rock, and it takes a considerable amount of differential rock movement for emplaced waste packages to experience any fault displacement-induced loads because of unfilled space and voids in backfill present in an emplacement drift.

6.3. APPROACH

Based on the assumptions made in Section 5, hypothetical fault orientations with respect to an emplacement drift shown in Figures 1 through 3 are used to aid in evaluating fault displacement effects on emplacement drifts.

Figure 1 illustrates a normal dip-slip fault that intersects an emplacement drift in the direction either parallel or perpendicular to the drift. For the normal fault, the hanging wall is elevated while the foot wall is depressed.

Similar to Figure 1, Figure 2 illustrates a reverse fault that intercepts an emplacement drift in the direction either parallel or perpendicular to the drift. Reverse faulting results in an elevated footwall and a depressed hanging wall.

Figure 3 shows a strike-slip fault that intercepts an emplacement drift at an angle with respect to the drift axis. Strike-slip faulting results in a horizontal offset between the hanging wall and footwall in the direction of strike.

In establishing these conceptual fault diagrams, the fault width is set to be zero, and the trace length is set to be infinite.

6.3.1. General

As is outlined in the development plan for this fault displacement analysis (CRWMS M&O 1999a), this analysis is aimed at evaluating the potential adverse effects of design basis fault displacement hazards on emplacement drifts that are to be located at a depth a few hundred meters below the ground surface. As the analysis focuses on the time period of postclosure, no evaluation will be made regarding the fault displacement effects on any ground support system that is installed in emplacement drifts, though the ground control system is considered to be an integral part of an emplacement drift. Consequently, any effects of fault displacement, whether from a normal fault or from a Reverse fault, on emplacement drifts are the same in principle. Subsequent evaluations are based on the normal and strike-slip fault scenarios.

When an earthquake occurs, the displacement or slip on the fault occurs in a few seconds. The displacement on the fault generates seismic waves that propagate through the surrounding rock. A significant portion of the stored elastic energy goes into the seismic waves; the remainder is dissipated as heat by friction on the fault. Therefore, the process leading to the fault displacement, excluding the fault displacement due to creep, is rather dynamic in nature. Quasi-static solutions to fault displacement are made. These solutions consider that the fault displacement is irreversible and that permanent changes in stress and displacement within the influence zone of the fault will take place accordingly.

It must be emphasized here that this analysis is not to discuss the fault displacement hazard but to evaluate the effects of fault displacement.

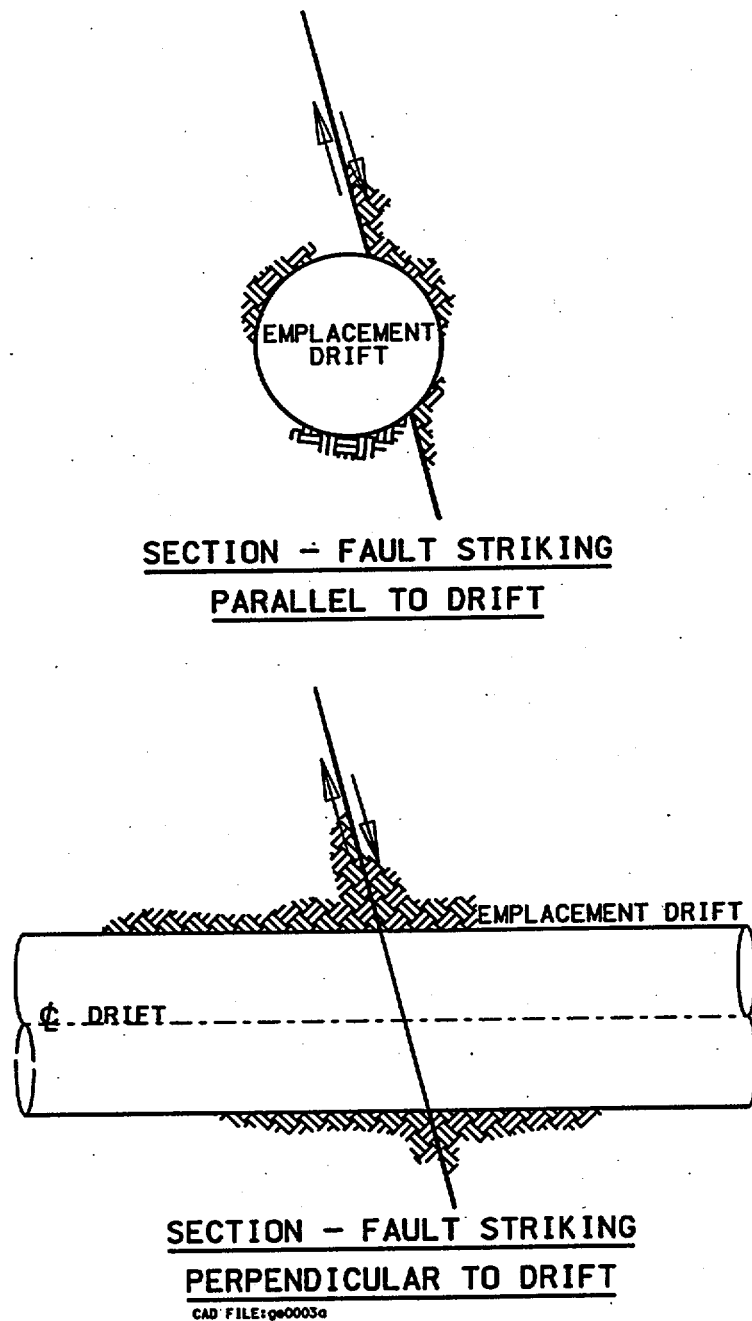


Figure 1. Normal Faulting Scenario

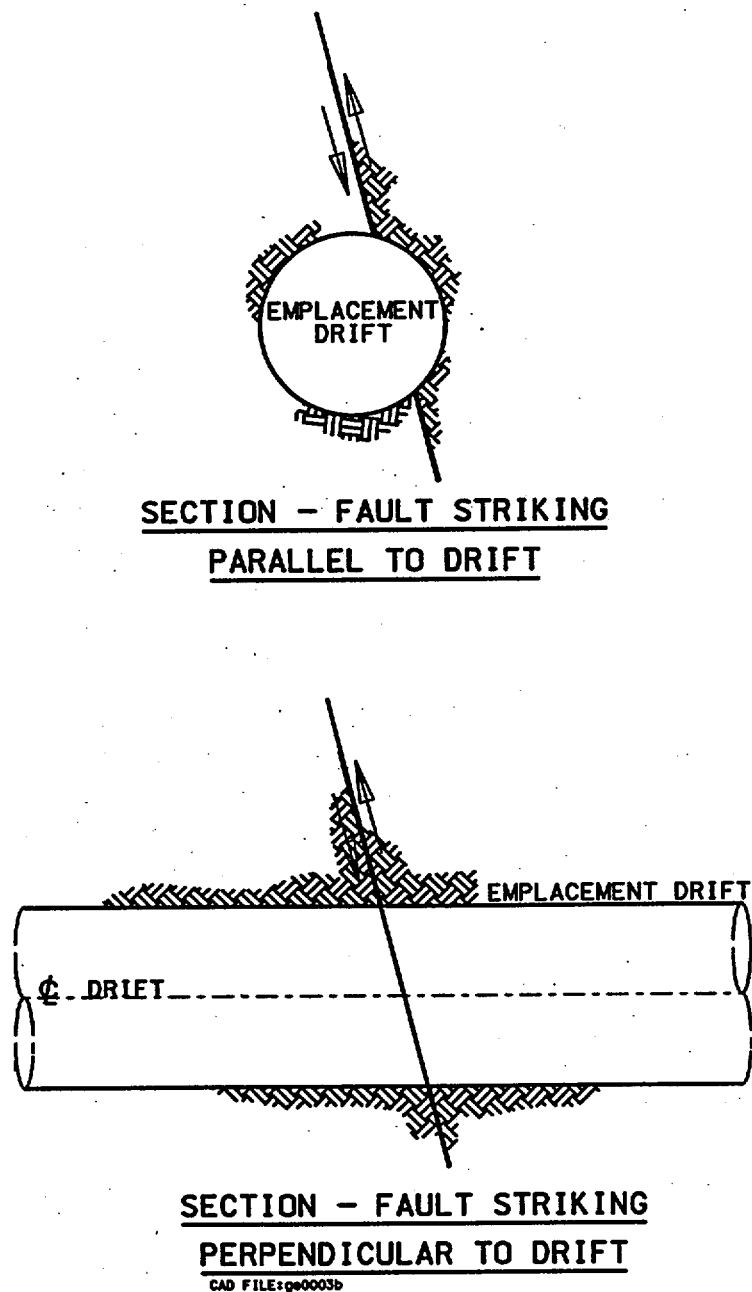


Figure 2. Reverse Faulting Scenario

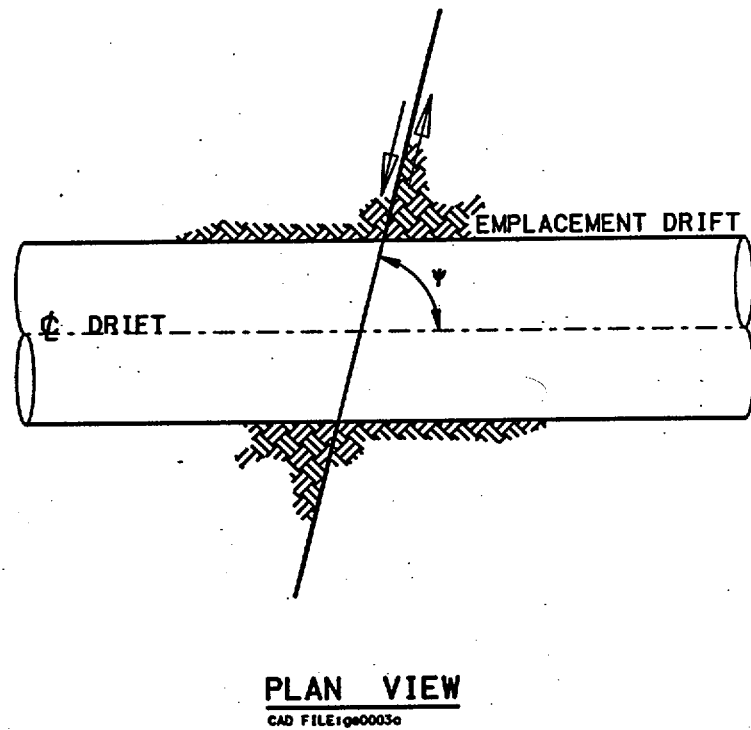


Figure 3. Strike-Slip Faulting Scenario

6.3.2. Analytical Approximation for Normal and Reverse Faults

A closed-form solution to the problem of a constant displacement discontinuity over a finite line segment in an infinite elastic solid (Crouch and Starfield 1983, pp. 80-84) is used to evaluate fault displacement effects. Figure 4 shows a sketch of the displacement discontinuity problem for which a closed-form solution has been developed. With constant displacement discontinuity components represented as D_x and D_y , displacements and stresses caused by the occurrence of D_x and D_y in the vicinity of the discontinuity are given as functions of position (x,y) in a Cartesian coordinate system, i.e.,

$$u_x = D_x[2(1-\nu)f_{,y} - yf_{,xx}] + D_y[-(1-2\nu)f_{,x} - yf_{,xy}] \quad (1)$$

$$u_y = D_x[(1-2\nu)f_{,x} - yf_{,xy}] + D_y[2(1-\nu)f_{,y} - yf_{,yy}] \quad (2)$$

$$\sigma_{xx} = 2GD_x(+2f_{,xy} + yf_{,xyy}) + 2GD_y(f_{,yy} + yf_{,yyy}) \quad (3)$$

$$\sigma_{yy} = 2GD_x(-yf_{,xyy}) + 2GD_y(f_{,yy} - yf_{,yyy}) \quad (4)$$

$$\sigma_{xy} = 2GD_x(f_{,yy} + yf_{,yyy}) + 2GD_y(-yf_{,xyy}) \quad (5)$$

where

u_x = displacement component in the x-axis direction (i.e., parallel to the discontinuity),

u_y = displacement component in the y-axis direction (i.e., perpendicular to the discontinuity),

σ_{xx} = normal stress in the x-axis direction,

σ_{yy} = normal stress in the y-axis direction,

σ_{xy} = shear stress in the x-y plane,

D_x = constant displacement jump parallel to the discontinuity,

D_y = constant displacement jump perpendicular to the discontinuity,

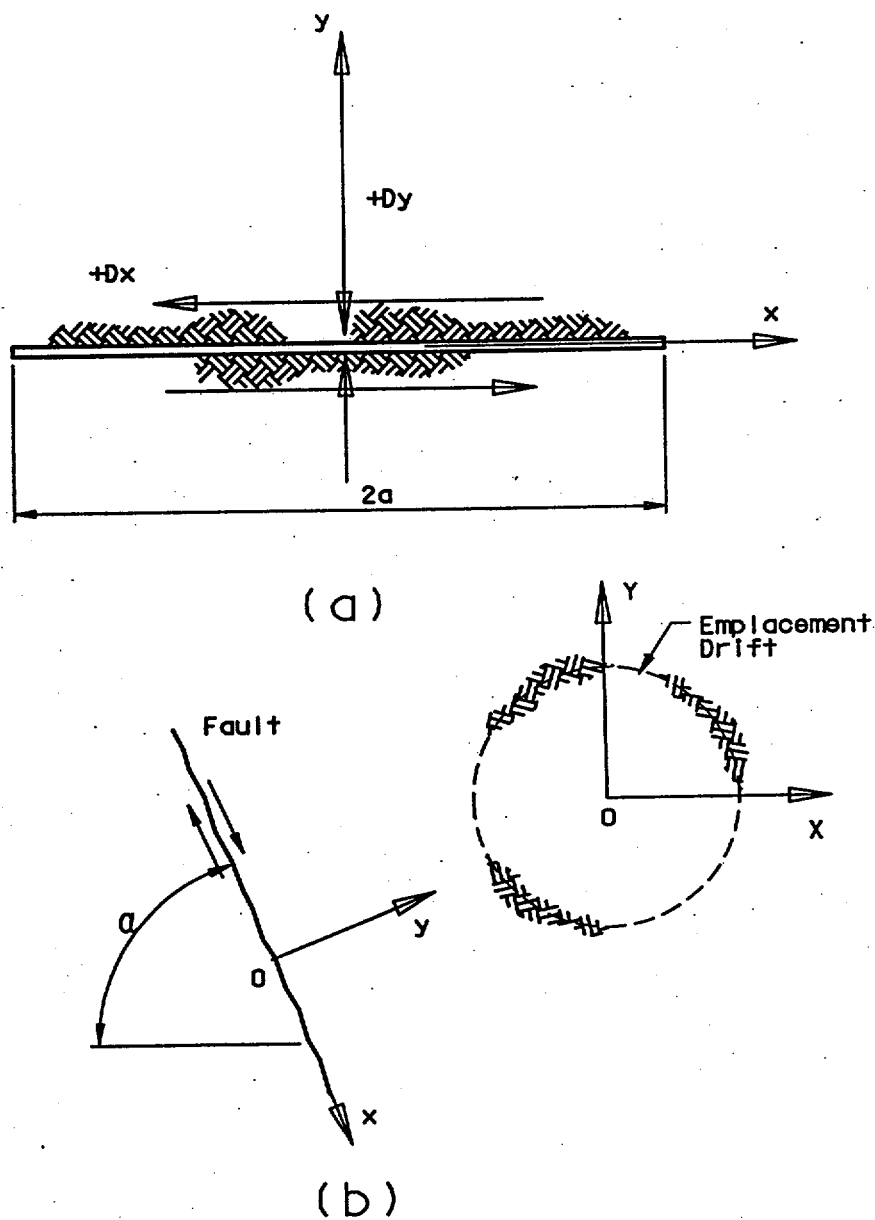
G = shear modulus of the medium where the displacement discontinuity occurs,

ν = Poisson's ratio of the medium where the displacement discontinuity occurs,

f = a function of x and y (to be described later in this section), and

$f_{,x}$, $f_{,y}$, $f_{,xx}$, $f_{,yy}$, $f_{,xy}$, $f_{,xyy}$, and $f_{,yyy}$ = derivatives of function $f(x,y)$ (to be defined later on in this section) through third order respectively.

Given D_x and D_y , expressions (1) through (5) can be solved for displacements and stresses at any given location (x, y) that is in the vicinity of this discontinuity. It should be reemphasized that displacements and stresses shown in the left sides of expressions (1) through (5) are induced in the medium by displacement discontinuities and have nothing to do with any preexisting stresses in the medium.



CAD FILE:ge0004o

Figure 4. Constant Displacement Discontinuity Concept Used for Fault Displacement Evaluation: (a) Mathematical Schematic for Closed-Form Solutions; (b) Application to the Emplacement Drift Vicinity.

By treating a fault as discontinuity, expressions (1) through (5) are used in this analysis to approximate the fault displacement effects which are expressed in terms of stress and displacement disturbances in the rock mass caused by a specified fault displacement. Once the analogue is mathematically drawn between a discontinuity and fault illustrated in Figure 4, D_y , being representative of the normal displacement (i.e., a separation or dilation between the hanging wall and foot wall of a fault), is discarded because such a fault separation is unrealistic. Furthermore, the depth of faulting is considered to be deep enough to validate the closed-form solutions which are based on an infinite solid (Assumption 5.10). Also, per Assumption 5.11, the dip angle of a fault is not considered. Therefore, D_x , being representative of the constant fault displacement (See Assumption 5.1) along the fault, is used only. By setting D_y to zero, expressions (1) through (5) are reduced to expressions (6) through (10).

$$u_x = D_x[2(1-\nu)f_{,y} - yf_{,xx}] \quad (6)$$

$$u_y = D_x[(1-2\nu)f_{,x} - yf_{,xy}] \quad (7)$$

$$\sigma_{xx} = 2GD_x(+2f_{,xy} + yf_{,xyy}) \quad (8)$$

$$\sigma_{yy} = 2GD_x(-yf_{,xyy}) \quad (9)$$

$$\sigma_{xy} = 2GD_x(f_{,yy} + yf_{,yyy}) \quad (10)$$

where

$$f(x,y) = -\{y \cdot \arctan[y/(x-a)] - y \cdot \arctan[y/(x+a)] \\ - (x-a) \ln\sqrt{(x-a)^2 + y^2} + (x+a) \ln\sqrt{(x+a)^2 + y^2}\} / [4\pi(1-\nu)] \quad (11)$$

$$f_{,x} = \{\ln\sqrt{(x-a)^2 + y^2} - \ln\sqrt{(x+a)^2 + y^2}\} / [4\pi(1-\nu)] \quad (12)$$

$$f_{,y} = -\{\arctan[y/(x-a)] - \arctan[y/(x+a)]\} / [4\pi(1-\nu)] \quad (13)$$

$$f_{,xy} = \{y/[(x-a)^2 + y^2] - y/[(x+a)^2 + y^2]\} / [4\pi(1-\nu)] \quad (14)$$

$$f_{,xx} = -f_{,yy} = \{(x-a)/[(x-a)^2 + y^2] - (x+a)/[(x+a)^2 + y^2]\} / [4\pi(1-\nu)] \quad (15)$$

$$f_{,xyy} = -f_{,xxx} = \{[(x-a)^2 - y^2]/[(x-a)^2 + y^2]^2 - [(x+a)^2 - y^2]/[(x+a)^2 + y^2]^2\} / [4\pi(1-\nu)] \quad (16)$$

$$f_{,yyy} = -f_{,xxy} = 2y\{(x-a)/[(x-a)^2 + y^2]^2 - (x+a)/[(x+a)^2 + y^2]^2\} / [4\pi(1-\nu)] \quad (17)$$

As is illustrated in Figure 4, the parameter "a" is viewed as half the fault length in the dip direction. The function and its derivatives have singularities at $x = \pm a$ and $y = 0$. These singular points correspond to both ends of a fault and will not have any consequence to the evaluation of fault displacement on emplacement drifts because the range of interest is $|x| < a$ and $|y| > 0$ where a fault does not terminate in the immediate vicinity of an emplacement drift.

In the next section (i.e., Section 6.4.1), induced stresses and displacements at an emplacement drift location will be calculated using expressions (6) through (9). The location of an emplacement drift relative to the fault is defined by x and y coordinates. Since Figure 4 corresponds to the scenario where the fault is parallel to the emplacement drift axis (See Assumption 5.2), the induced stresses and displacements at any given x and y coordinates are true along the entire drift. In other words, the results are independent of the direction of the drift axis as the fault is assumed to be infinitely long (Assumption 5.6). However, when a fault intersects an emplacement drift at a right angle (See Assumption 5.2), the induced stresses and displacements vary along the drift axis. The fault shown in Figure 4 has a planar surface with the zero fault zone width (Assumptions 5.4 and 5.5).

By varying the value of fault displacement D_x and fault extent "a", induced stresses and displacements are determined, and their effects are evaluated. Calculation details are shown in Section 6.4.1.

6.3.3. Analytical Approximation for Strike-Slip Faults

A strike-slip fault is characterized by its strictly-horizontal displacement along the fault. There is no strain in the vertical direction. The geodynamics textbook (Turcotte and Schubert 1982, p. 367) provides some elastic solutions for strike-slip faulting. By considering Assumptions 5.1 and 5.3, Figure 5 illustrates the simplified strike-slip fault for which analytical solutions are given in that textbook. Assumptions 5.4 through 5.6 are also used in establishing the conceptual diagram for a strike-slip fault. The following analytical expression for the stress induced by a simplified strike-slip fault is used to aid in evaluating the effects of fault displacement on emplacement drifts:

$$\sigma_{xz} = \sigma_{xz,0}y/(y^2-a^2)^{1/2} \text{ (for } y>a; \text{ otherwise, } \sigma_{xz} = 0) \quad (18)$$

where

$\sigma_{xz,0}$ = initial shear stress which is related to the surface fault displacement by

$$\sigma_{xz,0} = \Delta w_{z0} * G/2a \text{ (}\Delta w_{z0} \text{ is the surface fault displacement)}$$

a = the depth of crack induced for representing a strike-slip fault

G = shear modulus of the rock

y = depth of interest. For this analysis, it is a drift location relative to the fault.

σ_{xz} = resultant shear stresses after introducing the crack along the fault

It must be pointed out that expression (18) has rather limited application towards evaluating the effects from a strike-slip fault. It will not allow for considering the horizontal offset of an emplacement drift with respect to the fault, as the x-coordinate has been set to zero. For the same reason, the vertical distance is only considered. By considering an emplacement drift that is directly located underneath a steeply-dipping strike-slip fault, expression (18) will allow for approximating the shear stress to be caused by fault displacement.

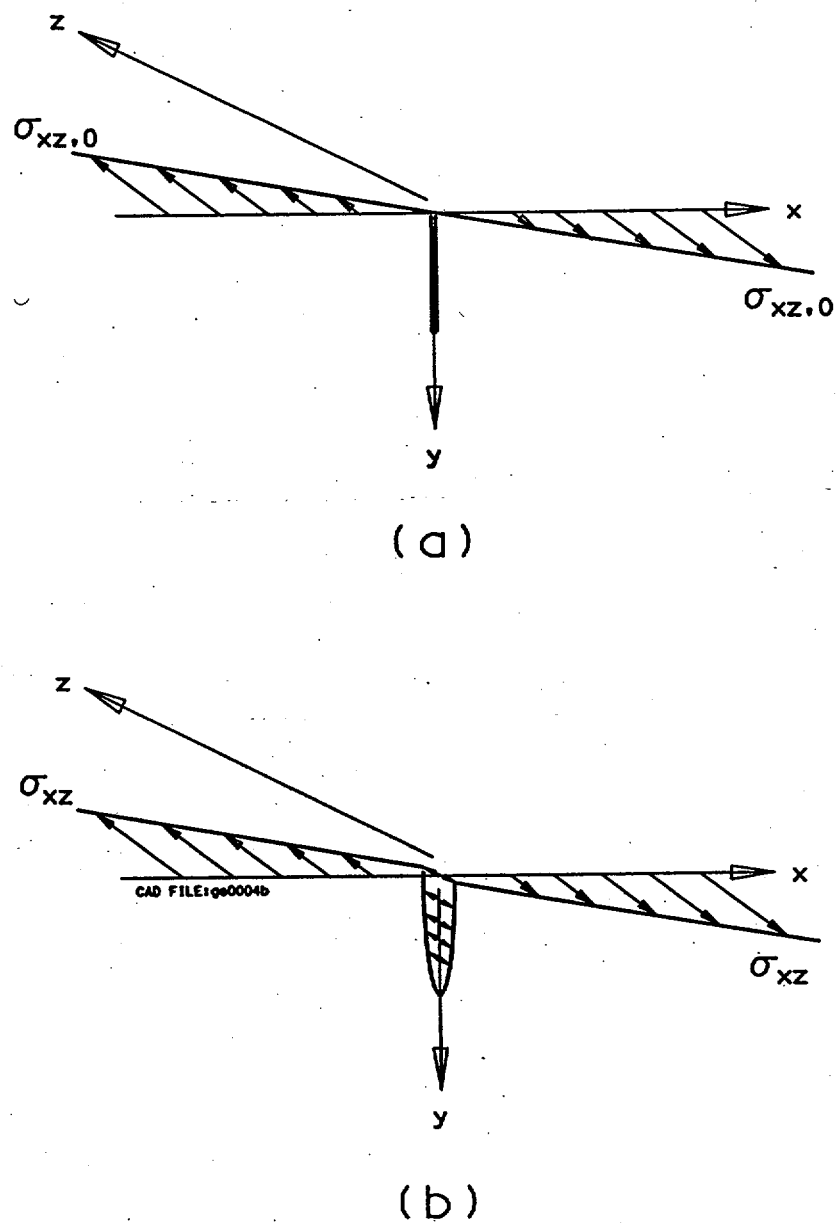


Figure 5. Simplified Strike-Slip Fault Diagram: (a) Prior to Faulting; (b) After Faulting

6.4. EVALUATION OF FAULT DISPLACEMENT EFFECTS

This section evaluates the effects of fault displacement on emplacement drifts. These effects are expressed in terms of displacement and stress changes caused by fault displacement. The analytical expressions discussed earlier in Section 6.3.1 are used.

6.4.1. Normal and Reverse Faulting Scenarios

Calculation of induced displacements and stresses by using expressions (7) through (10) requires the determination of derivatives defined by expressions (12) through (17). The location of an emplacement drift relative to the fault is defined by x and y coordinates. Since the derivatives are algebraic functions of x and y with singularities at $x = \pm a$ and $y = 0$, *Microsoft Excel 97* is used to aid in performing the calculation and illustrating the results graphically.

6.4.1.1 Verification of Routine Results

Hand calculation of a few test cases is performed to verify that the routine provides correct results for displacement (u_x) and shear stress (σ_{xy}) over the range of input parameters presented below:

$a = 100$ and 400 m respectively (Section 5.8)

$x = 0$

$y = 0$ and 100 m respectively (Section 5.7)

$D_x = 0.001$ m = 1 mm (Displacement value selected for test cases)

$\nu = 0.21$ (Section 4.1)

$G = 0.5E/(1+\nu) = 0.5 \times 8.98$ (GPa)/(1+0.21) = 3.71 GPa (E value is given in Section 4.1)

Used for calculation of u_x and σ_{xy}

By setting x to 0 , i.e., a scenario where an emplacement drift bisects the fault in distance, lengthy derivative expressions (12) through (17) are reduced to the following:

$$f_{,x} |_{x=0} = 0 \quad (19)$$

$$f_{,y} |_{x=0} = [\arctan(y/+a) - \arctan(y/-a)] / [4\pi(1-\nu)] \quad (20)$$

$$f_{,xy} |_{x=0} = 0 \quad (21)$$

$$f_{,xx} |_{x=0} = -f_{,yy} |_{x=0} = -2a/(a^2 + y^2) / [4\pi(1-\nu)] \quad (22)$$

$$f_{,xyy} |_{x=0} = -f_{,xxx} |_{x=0} = 0 \quad (23)$$

$$f_{,yyy} |_{x=0} = -f_{,xxy} |_{x=0} = -4a\{y/[a^2 + y^2]^2\} / [4\pi(1-\nu)] \quad (24)$$

With $x=0$ this renders u_y , σ_{xx} and σ_{yy} to be zero regardless of the distance from an emplacement drift to the fault. The following hand calculations are used to verify the routine results. The routine results (presented in Table 3) are reproduced from the Microsoft Excel spreadsheet where

displacement is designated "ux(mm)" and shear stress is designated "sigxy(MPa)." These results are considered verified if they are duplicated by hand calculations over the range of inputs.

For the displacement case "ux(mm)" four results are calculated (a=100, y=0; a=400, y=0; a=100, y=100; and a=400, y=100):

$$\begin{aligned} u_x(x=0, y=0) |_{a=100} &= D_x[2(1-\nu)f_{,y} - yf_{,xx}] \\ &= 0.001 \{2x(1-0.21)x[\arctan(0/100) - \arctan(0/-100)] - 0*f_{,xx}\} / [4\pi(1-0.21)] \\ &= 0.001x[2x(1-0.21)(0-\pi)-(0)] / [4\pi(1-0.21)] \\ &= -0.0005 \text{ (m)} = -0.5 \text{ (mm)} \end{aligned}$$

$$\begin{aligned} u_x(x=0, y=0) |_{a=400} &= D_x[2(1-\nu)f_{,y} - yf_{,xx}] \\ &= 0.001 \{2x(1-0.21)x[\arctan(0/400) - \arctan(0/-400)] - 0*f_{,xx}\} / [4\pi(1-0.21)] \\ &= 0.001x[2x(1-0.21)(0-\pi)-(0)] / [4\pi(1-0.21)] \\ &= -0.0005 \text{ (m)} = -0.5 \text{ (mm)} \end{aligned}$$

$$\begin{aligned} u_x(x=0, y=100) |_{a=100} &= D_x[2(1-\nu)f_{,y} - yf_{,xx}] \\ &= 0.001 \{2x(1-0.21)x[\arctan(100/100) - \arctan(100/-100)] \\ &\quad - 100*(-2*100)/(100^2 + 100^2)\} / [4\pi(1-0.21)] \\ &= 0.001x[2x(1-0.21)x(\pi/4 - 3\pi/4)+1] / [4\pi(1-0.21)] \\ &= -0.000149 \text{ (m)} = -0.149 \text{ (mm)} \end{aligned}$$

$$\begin{aligned} u_x(x=0, y=100) |_{a=400} &= D_x[2(1-\nu)f_{,y} - yf_{,xx}] \\ &= 0.001 \{2x(1-0.21)x[\arctan(100/400) - \arctan(100/-400)] \\ &\quad - 400*(-2*100)/(100^2 + 400^2)\} / [4\pi(1-0.21)] \\ &= 0.001x2x(1-0.21)[(0.244978-2.89661)+0.47059] / [4\pi(1-0.21)] \\ &= -0.0003746 \text{ (m)} = -0.3746 \text{ (mm)} \end{aligned}$$

For the shear stress case "sigxy(MPa)" four results are calculated (a=100, y=0; a=400, y=0; a=100, y=100; and a=400, y=100):

$$\begin{aligned} \sigma_{xy}(x=0, y=0) |_{a=100} &= 2GD_x(f_{,yy} + yf_{,yyy}) \\ &= 2x3.71x10^9x0.001 \{[2x100/(100^2 + 0^2)] + 0*f_{,yyy}\} / [4\pi(1-0.21)] \\ &= 0.0149 \text{ (MPa)} \end{aligned}$$

$$\begin{aligned} \sigma_{xy}(x=0, y=0) |_{a=400} &= 2GD_x(f_{,yy} + yf_{,yyy}) \\ &= 2x3.71x10^9x0.001 \{[2x400/(400^2 + 0^2)] + 0*f_{,yyy}\} / [4\pi(1-0.21)] \\ &= 0.0037 \text{ (MPa)} \end{aligned}$$

$$\begin{aligned} \sigma_{xy}(x=0, y=100) |_{a=100} &= 2GD_x(f_{,yy} + yf_{,yyy}) \\ &= 2x3.71x10^9x0.001 \{[2x100/(100^2 + 100^2)] \\ &\quad + 100x(-4x100)x[100/(100^2 + 100^2)^2]\} / [4\pi(1-0.21)] \\ &= 0 \end{aligned}$$

$$\begin{aligned}\sigma_{xy}(x=0,y=100)|_{a=400} &= 2GD_x(f_{,yy} + yf_{,yyy}) \\ &= 2 \times 3.71 \times 10^9 \times 0.001 \{ [2 \times 400 / (400^2 + 100^2)] \\ &\quad + 100x(-4 \times 400)x[100 / (400^2 + 100^2)^2] / [4\pi(1-0.21)] \} \\ &= 0.0031 \text{ (MPa)}\end{aligned}$$

Spreadsheet values are shown in Table 3 with the corresponding routine results bolded. The routine results were duplicated by hand calculations. Therefore, the routine is considered verified for use in subsequent computations.

Analytical results of the routine graphically presented in this analysis were constructed using standard *Microsoft Excel* graphing functions which can be visually verified. Absolute values of induced displacements are adopted in order to plot in logarithm scales.

Table 3. Selected Spreadsheet Results for Comparing Hand Calculations

a (m)	100	400	100	400
G (GPa)	3.71E+09	3.71E+09	3.71E+09	3.71E+09
v	0.21	0.21	0.21	0.21
Dx (m)	0.001	0.001	0.001	0.001
x (m)	0	0	0	0
y (m)	0	0	100	100
k=4*pi*(1-v)	9.9274244	9.9274244	9.9274244	9.9274244
(x-a)^2+y^2	10000	160000	20000	170000
(x+a)^2+y^2	10000	160000	20000	170000
x-a	-100	-400	-100	-400
x+a	100	400	100	400
(x-a)^2-y^2	10000	160000	0	150000
(x+a)^2-y^2	10000	160000	0	150000
f,x	0	0	0	0
f,y	-0.316455964	-0.31645596	-0.15822798	-0.26710204
f,xy	0	0	0	0
f,xx	-0.002014621	-0.00050366	-0.00100731	-0.00047403
f,yy	0.002014621	0.00050366	0.00100731	0.00047403
f,xyy	0	0	0	0
f,xxx	0	0	0	0
f,yyy	0	0	-1.0073E-05	-5.5768E-07
f,xyy	0	0	1.0073E-05	5.5768E-07
ux(mm)	-0.500000422	-0.50000042	-0.14926915	-0.37461837
uy(mm)	0	0	0	0
sigxx(MPa)	0	0	0	0
sigyy(MPa)	0	0	0	0
sigxy(MPa)	0.01494849	0.00373712	0	0.00310349

6.4.1.2 Induced Displacements and Stresses

In the following, evaluation of stress and displacement disturbances caused by a fault displacement focuses on u_x , σ_{xx} and σ_{xy} because u_y and σ_{yy} are negligible when $D_y = 0$. Parameters listed in Section 4.1 and assumptions listed in Section 5 are used. Figures 6 through 21 show the induced displacements and stresses obtained by considering a variety of combinations of input parameters. Table 4 provides a road map showing all the input parameters used to produce each figure.

Table 4. Input Parameters for Spreadsheet Calculations

Figure	What for	RMQ	G (GPa)	ν	a (m)	Dx (mm)	x (m)	y (m)
6	u_x	-	-	0.21	100	1 - 1000	0	0 - 100
7	u_x	-	-	0.21	400	1 - 1000	0	0 - 100
8	σ_{xx}	1	3.71	0.21	100 - 400	1 - 1000	50	10
9	σ_{xx}	1	3.71	0.21	100 - 400	1 - 1000	50	60
10	σ_{xx}	1	3.71	0.21	100 - 400	1 - 1000	50	100
11	σ_{xx}	5	10.21	0.21	100 - 400	1 - 1000	50	10
12	σ_{xx}	5	10.21	0.21	100 - 400	1 - 1000	50	60
13	σ_{xx}	5	10.21	0.21	100 - 400	1 - 1000	50	100
14	σ_{xy}	1	3.71	0.21	100 - 400	1 - 1000	0	0
15	σ_{xy}	1	3.71	0.21	100 - 400	1 - 1000	0	10
16	σ_{xy}	1	3.71	0.21	100 - 400	1 - 1000	0	60
17	σ_{xy}	1	3.71	0.21	200 - 400	1 - 1000	0	100
18	σ_{xy}	5	10.21	0.21	100 - 400	1 - 1000	0	0
19	σ_{xy}	5	10.21	0.21	100 - 400	1 - 1000	0	10
20	σ_{xy}	5	10.21	0.21	100 - 400	1 - 1000	0	60
21	σ_{xy}	5	10.21	0.21	200 - 400	1 - 1000	0	100

Figures 6 and 7 show the rock movement at the emplacement drift location vs. fault displacement. Figure 6 corresponds to the $a = 100$ m case while Figure 7 corresponds to the $a = 400$ m case. As expected, the $y = 0$ scenario which represents direct intersection of a fault with an emplacement drift leads to the greatest rock movement in comparison to other scenarios where emplacement drifts are away from the fault. The predicted rock movement at an emplacement drift location diminishes rather slowly with the distance away from the fault. It can be seen from expressions (6) and (7) that only the Poisson's ratio enters the expressions. Since the Poisson's ratio value remains the same (Section 4.1) for all rock mass categories within the TSw2 thermal/mechanical unit, the rock movement predicted in Figures 6 and 7 is independent of rock mass categories.

The normal stress component induced at the emplacement drift location by fault displacement is shown in Figures 8 through 13. Figures 8 through 10 correspond to the RMQ = 1 category and Figures 11 through 13 correspond to the RMQ = 5 category. The induced stress is linearly proportional to the shear modulus of the rock mass. Evaluation results indicates that fault displacement has to be in the order of hundredths of meter in order to induce a normal stress disturbance of over 1 MPa. Generally speaking, an increase in stress by 1 MPa is considered to be insignificant compared either to the excavation-induced stress concentration or to thermally-induced stress in the vicinity of an emplacement drift.

Similar to the normal stress, the induced shear stress at the emplacement drift location by fault displacement is shown in Figures 14 through 21. Figures 14 through 17 correspond to RMQ category 1 and Figures 18 through 21 correspond to RMQ category 5. It is noted that the $a = 100$ m scenario is not presented in Figure 17 or 21 because the scenario leads to zero for the induced shear stress when $y = 100$ m, resulting in the removal of the scenario because of the logarithmic scale. In comparison to the induced normal stress at the emplacement drift location, the shear stress induced by fault displacement is much more pronounced, though its magnitude is still insignificant when the fault displacement occurs within a range of a few millimeters.

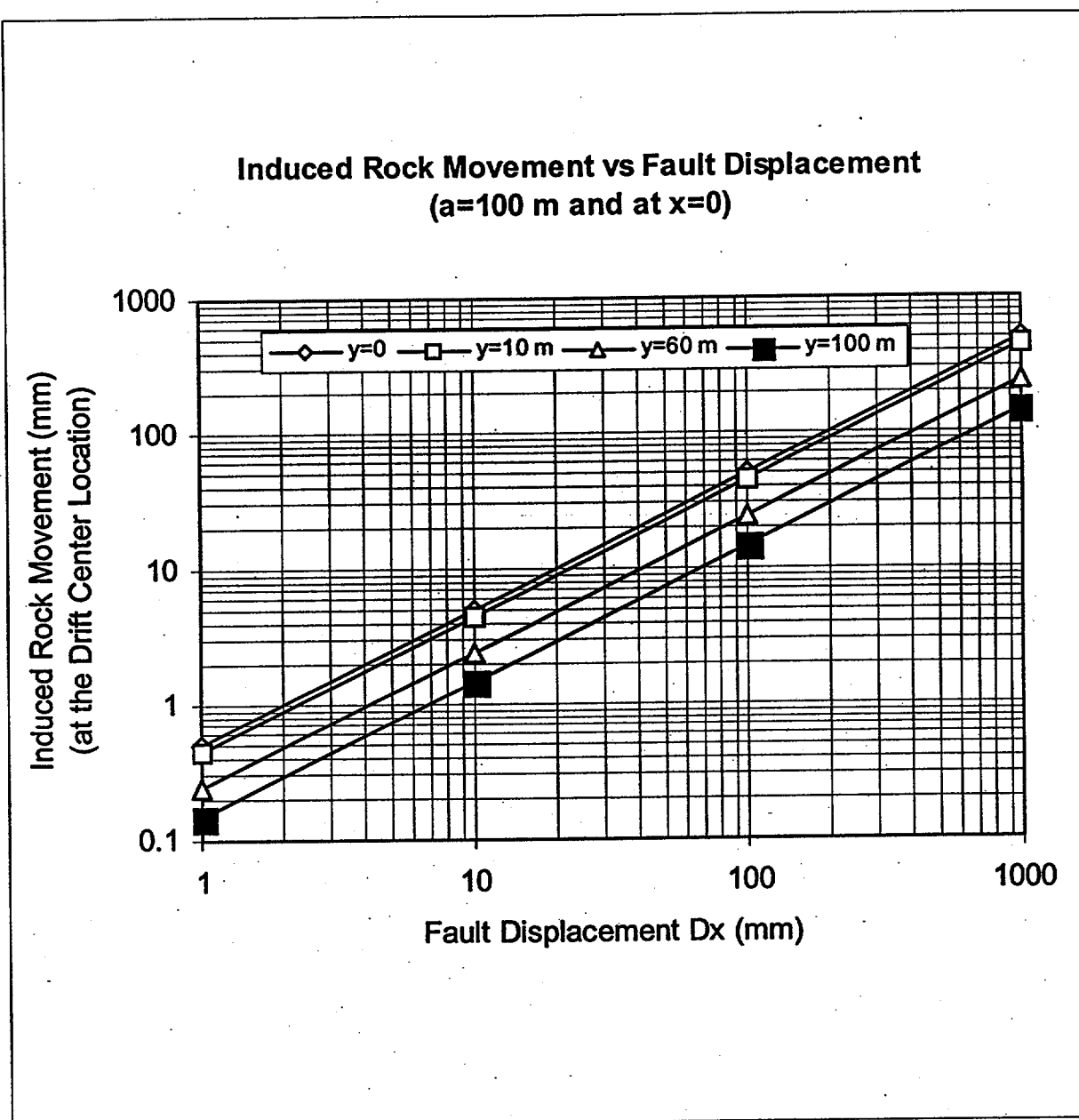


Figure 6. Induced Rock Movement at the Location of an Emplacement Drift vs. Fault Displacement with Half of the Fault Extent Equal to 100 m along the Dip

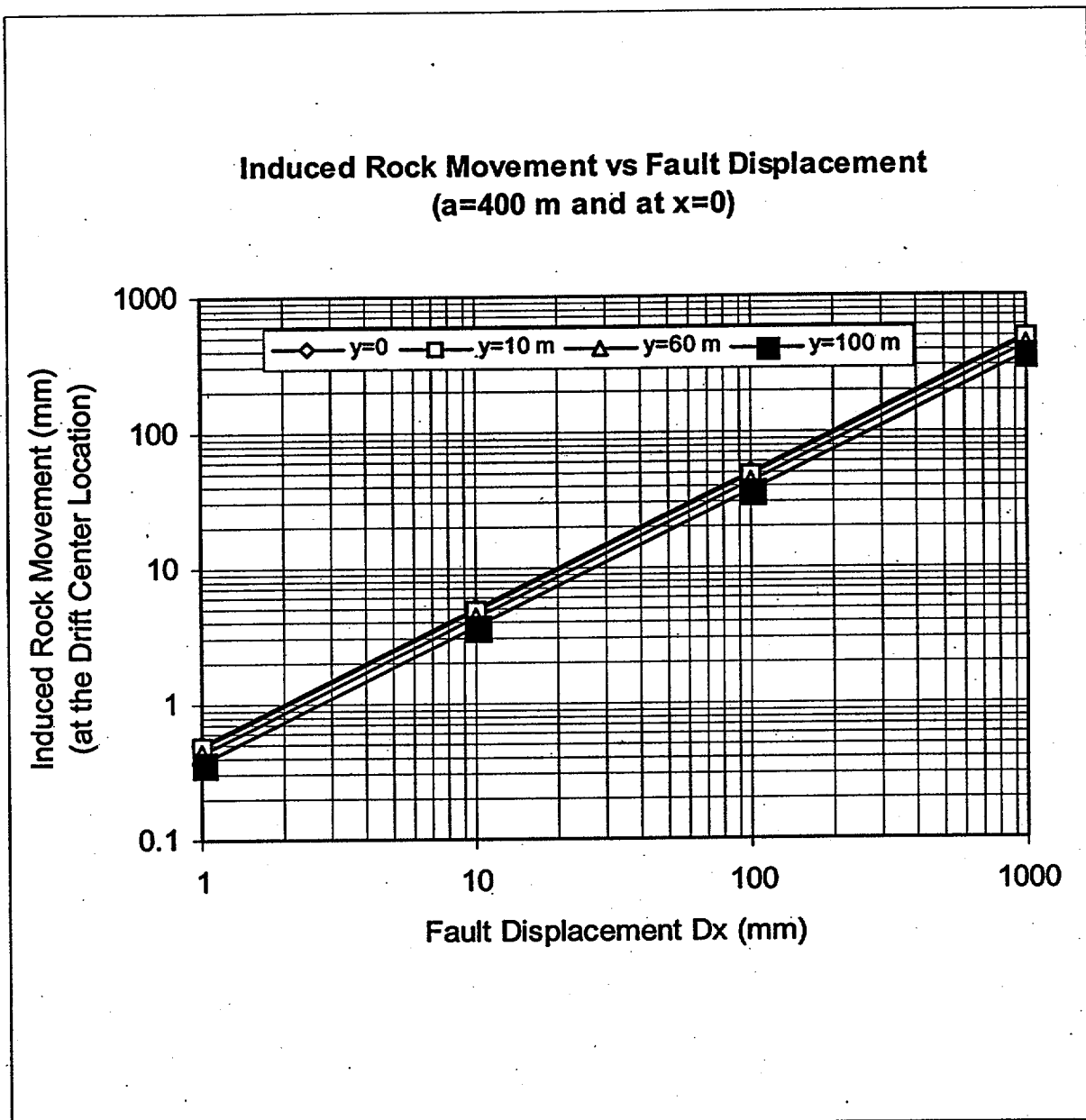


Figure 7. Induced Rock Movement at the Location of an Emplacement Drift vs. Fault Displacement with Half of the Fault Extent Equal to 400 m along the Dip

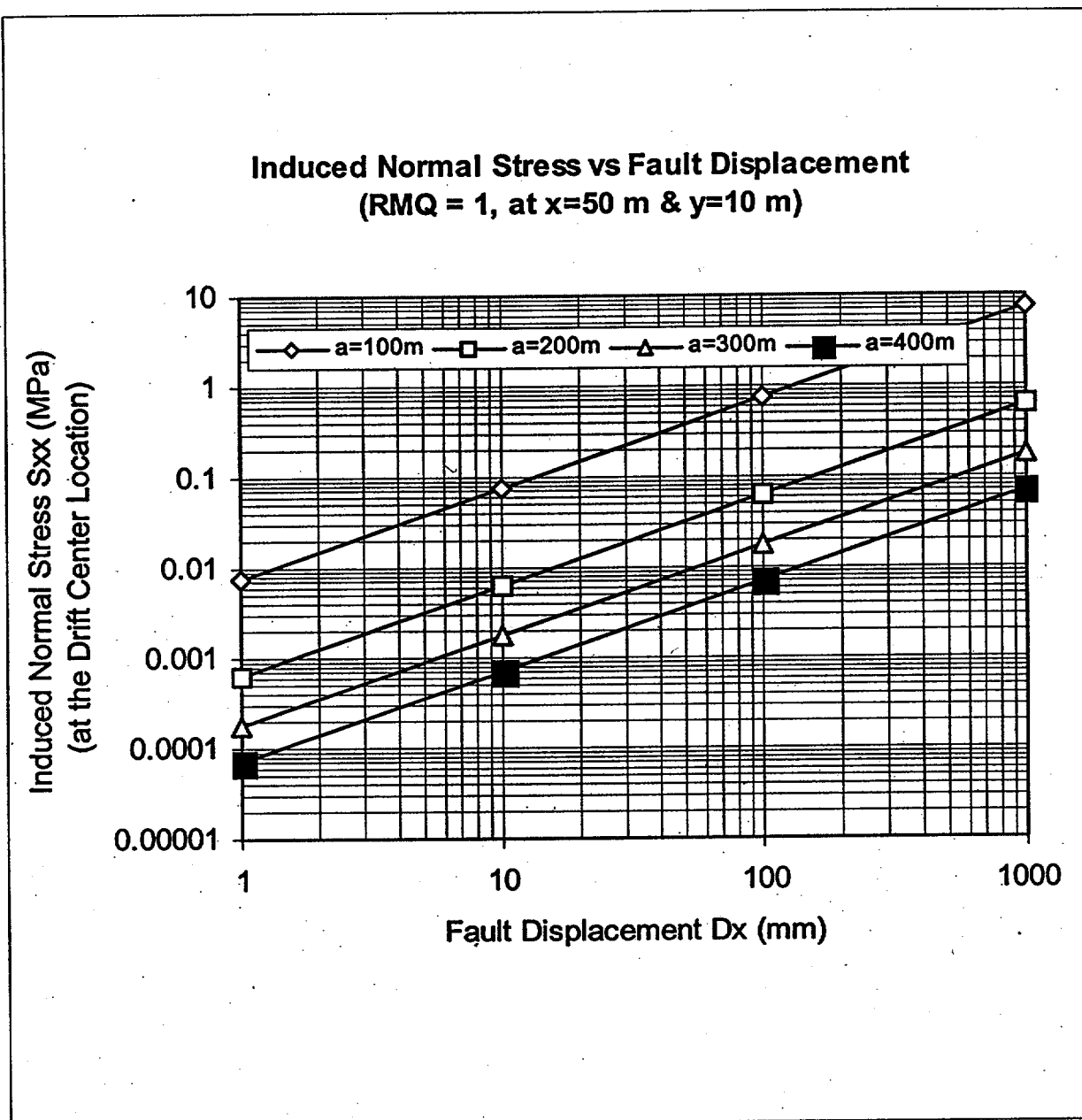


Figure 8. Induced Normal Stress at the Location of an Emplacement Drift vs. Fault Displacement: RMQ = 1, Distance between the Drift and Fault = 10 m.

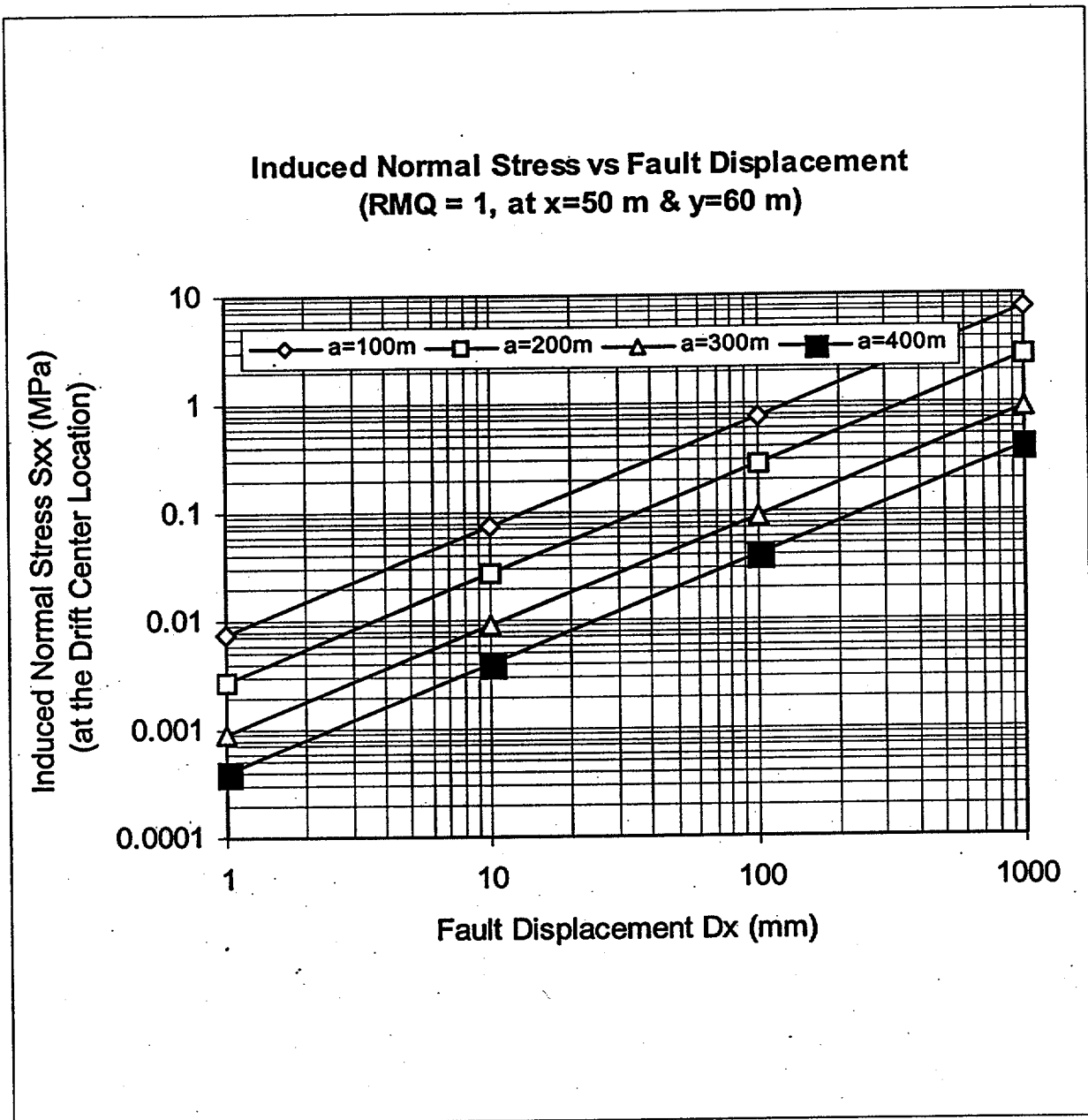


Figure 9. Induced Normal Stress at the Location of an Emplacement Drift vs. Fault Displacement: RMQ = 1, Distance between the Drift and Fault = 60 m.

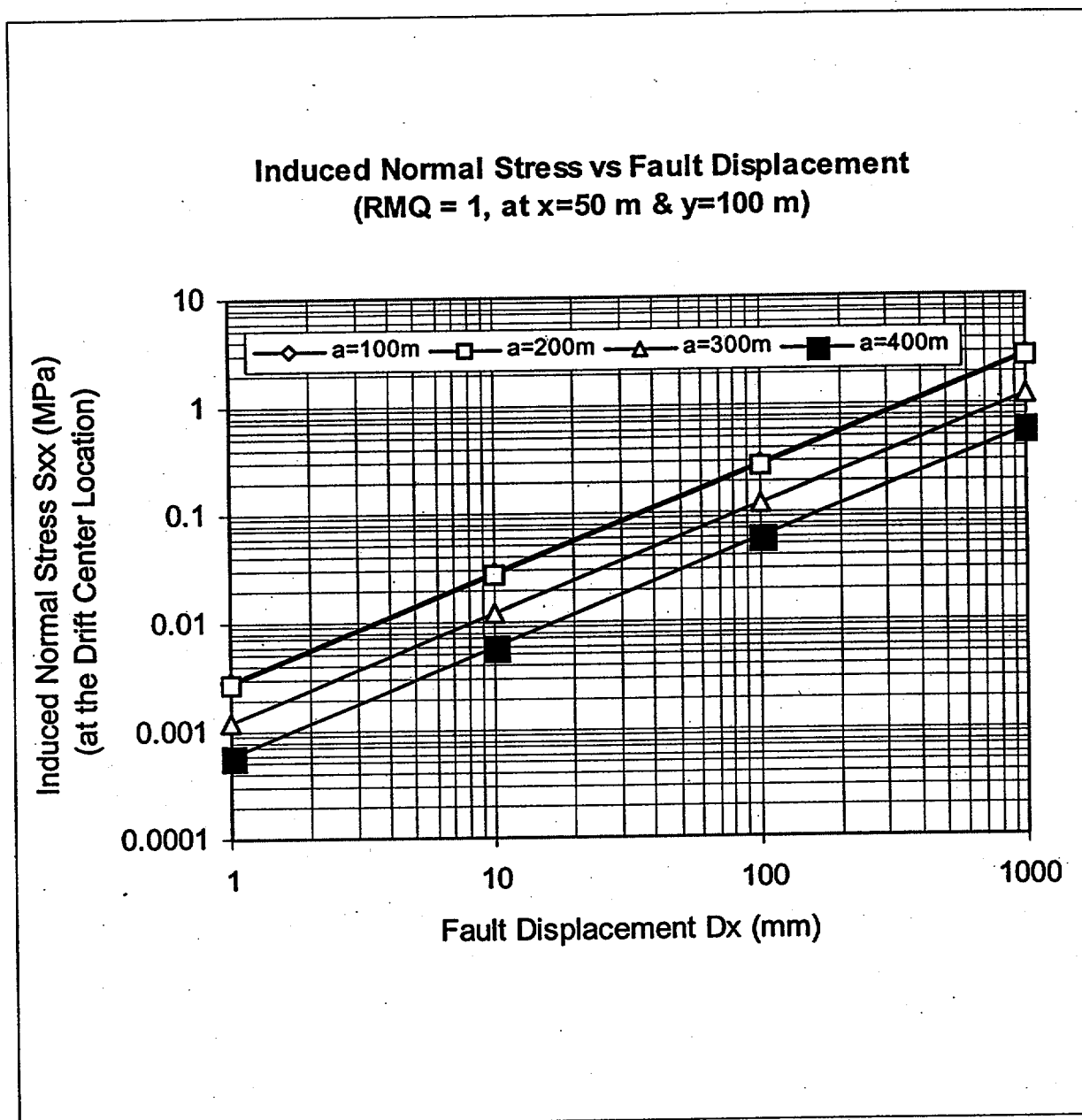


Figure 10. Induced Normal Stress at the Location of an Emplacement Drift vs. Fault Displacement: RMQ = 1, Distance between the Drift and Fault = 100 m.

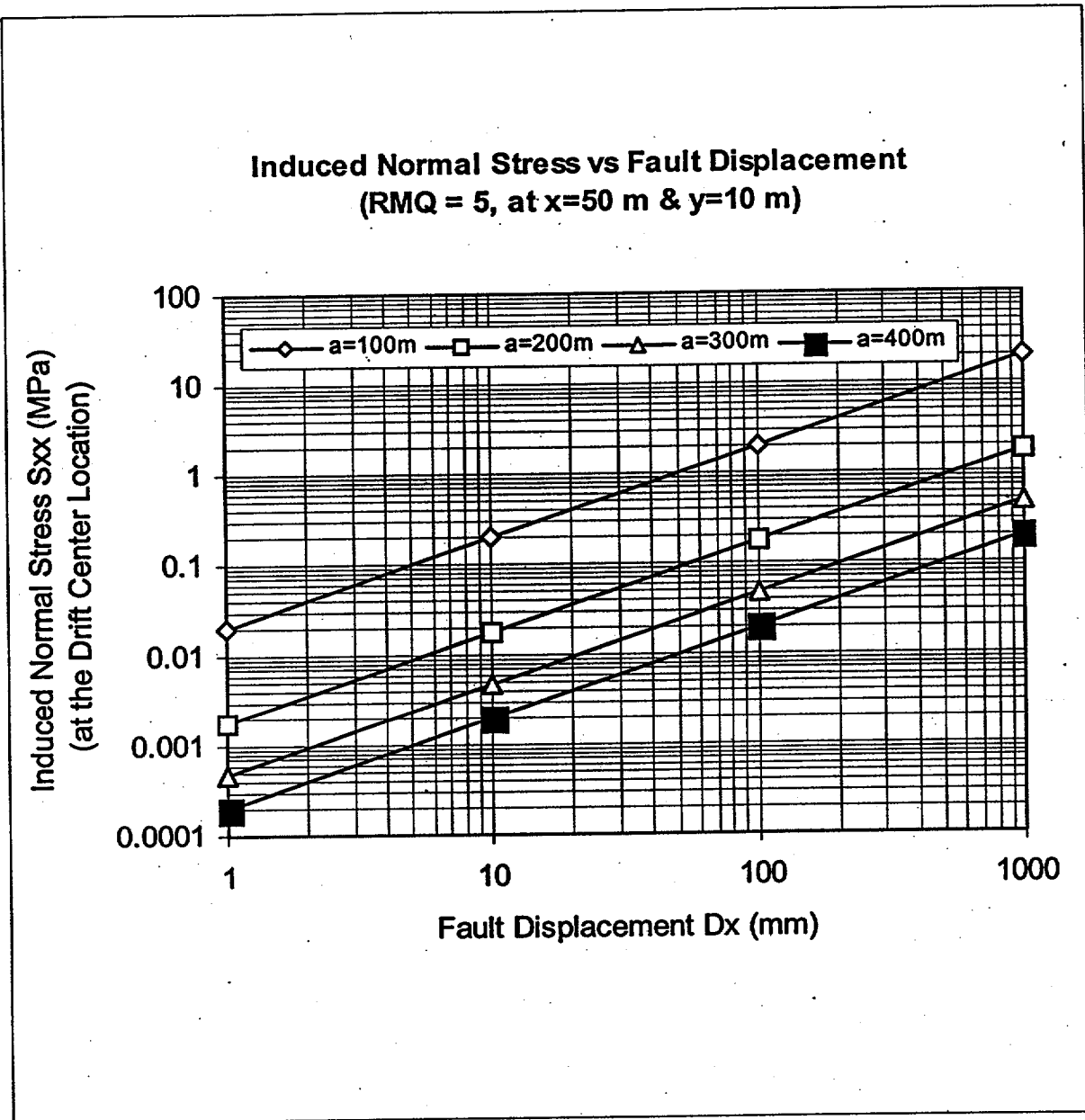


Figure 11. Induced Normal Stress at the Location of an Emplacement Drift vs. Fault Displacement: RMQ = 5, Distance between the Drift and Fault = 10 m.

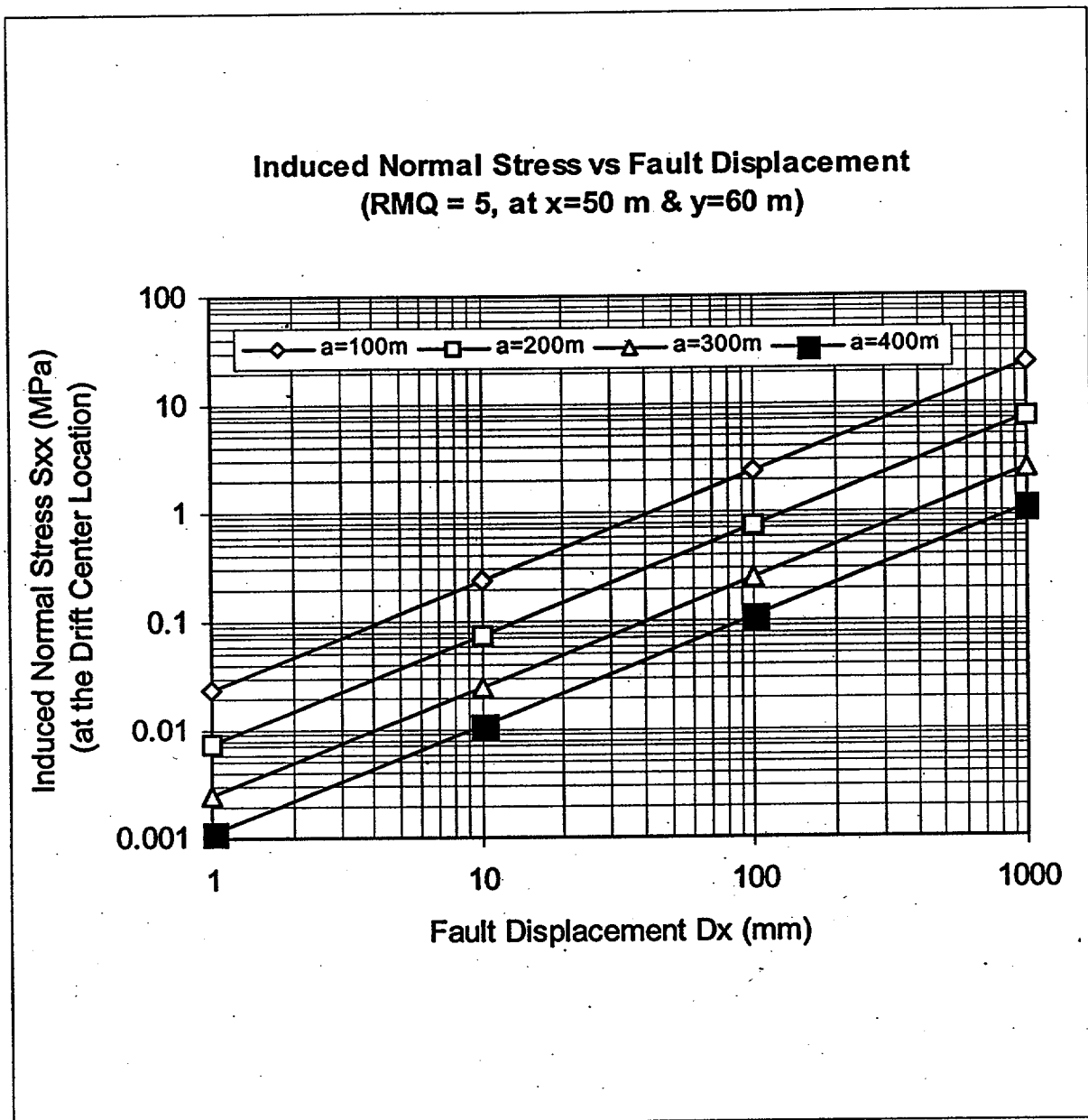


Figure 12. Induced Normal Stress at the Location of an Emplacement Drift vs. Fault Displacement: RMQ = 5, Distance between the Drift and Fault = 60 m.

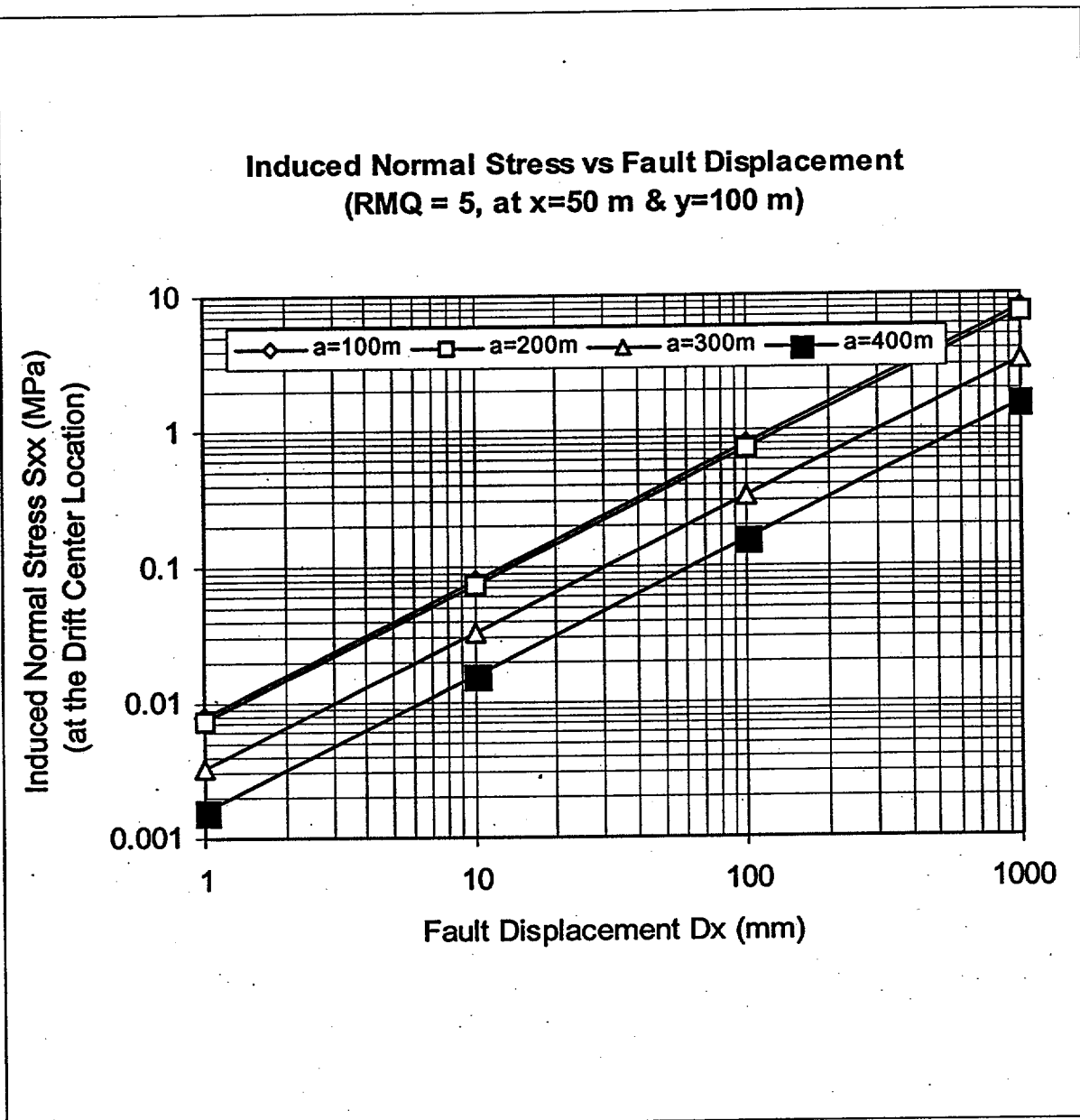


Figure 13. Induced Normal Stress at the Location of an Emplacement Drift vs. Fault Displacement:
RMQ = 1, Distance between the Drift and Fault = 100 m.

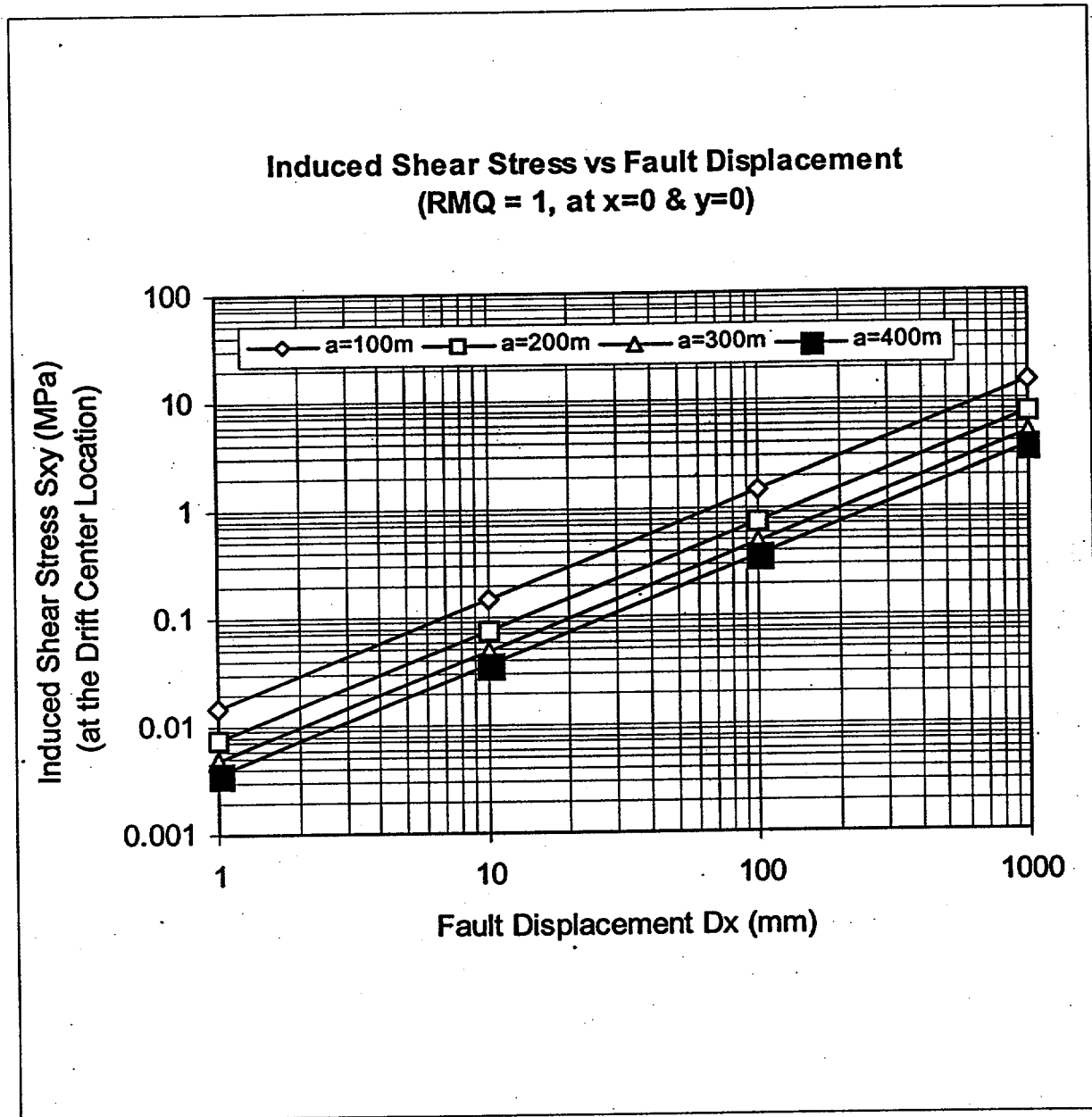


Figure 14. Induced Shear Stress at the Location of an Emplacement Drift vs. Fault Displacement:
RMQ = 1, Distance between the Drift and Fault = 0 m.

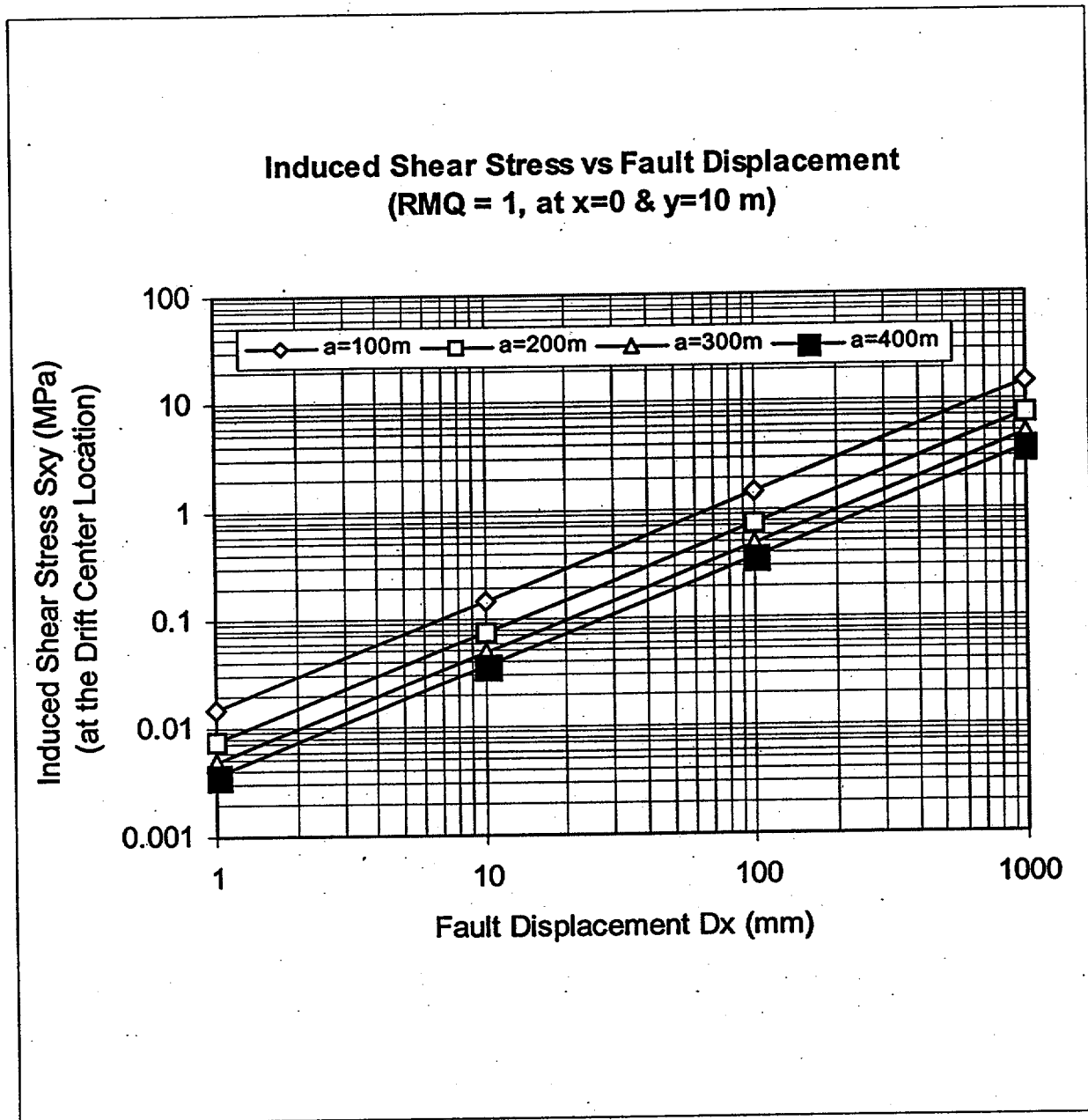


Figure 15. Induced Shear Stress at the Location of an Emplacement Drift vs. Fault Displacement: RMQ = 1, Distance between the Drift and Fault = 10 m.

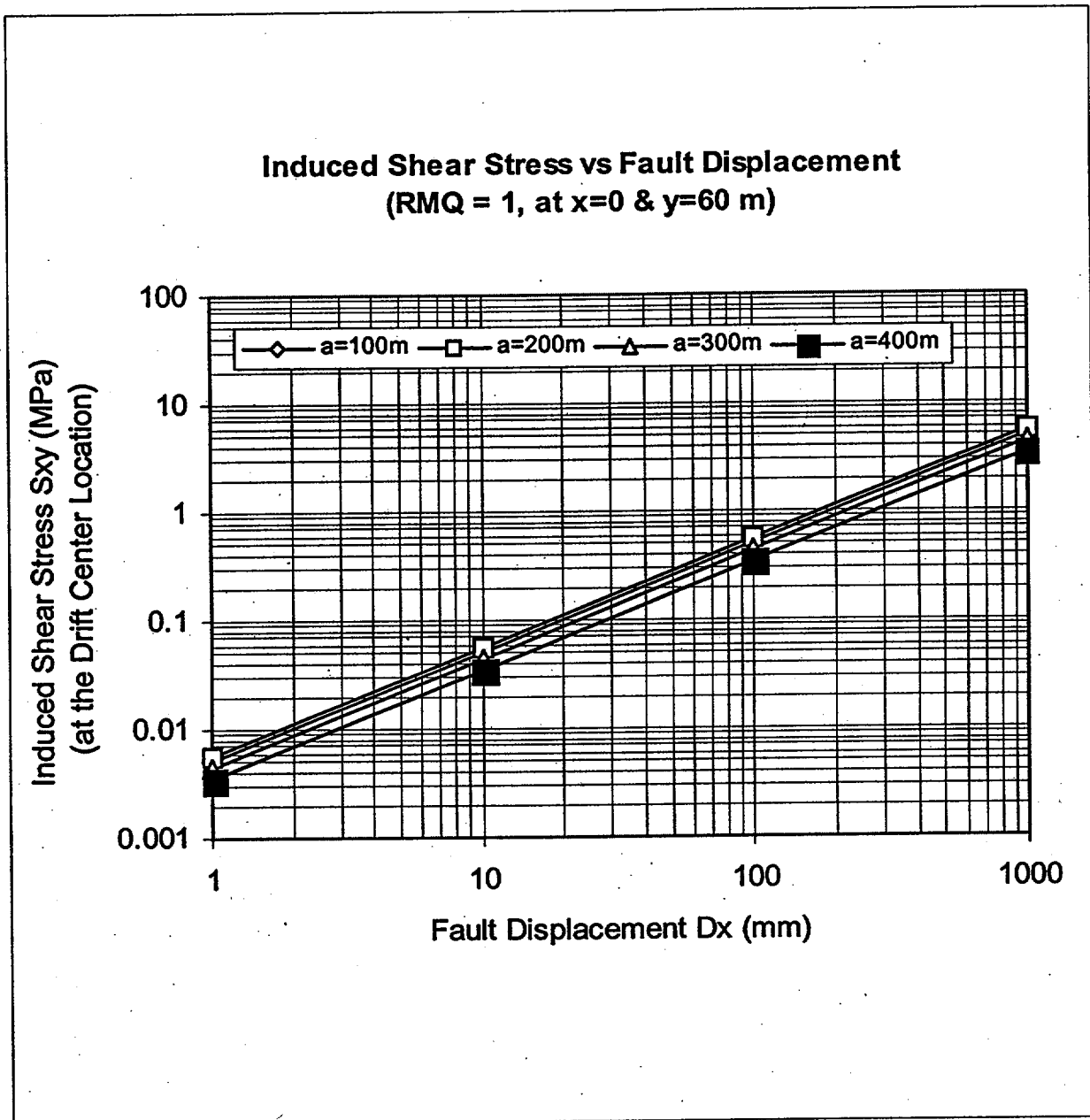


Figure 16. Induced Shear Stress at the Location of an Emplacement Drift vs. Fault Displacement: RMQ = 1, Distance between the Drift and Fault = 60 m.

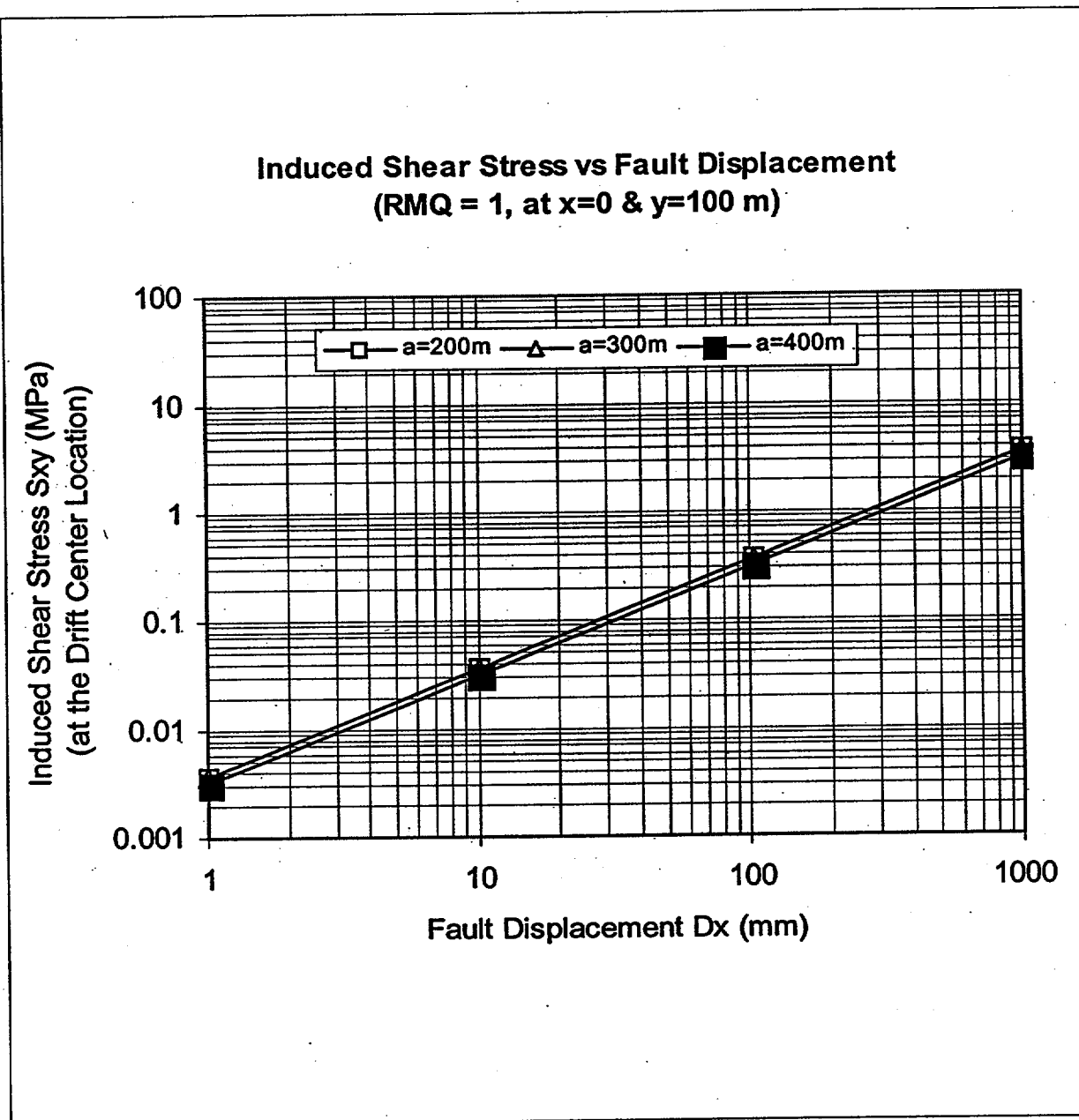


Figure 17. Induced Shear Stress at the Location of an Emplacement Drift vs. Fault Displacement: RMQ = 1, Distance between the Drift and Fault = 100 m.

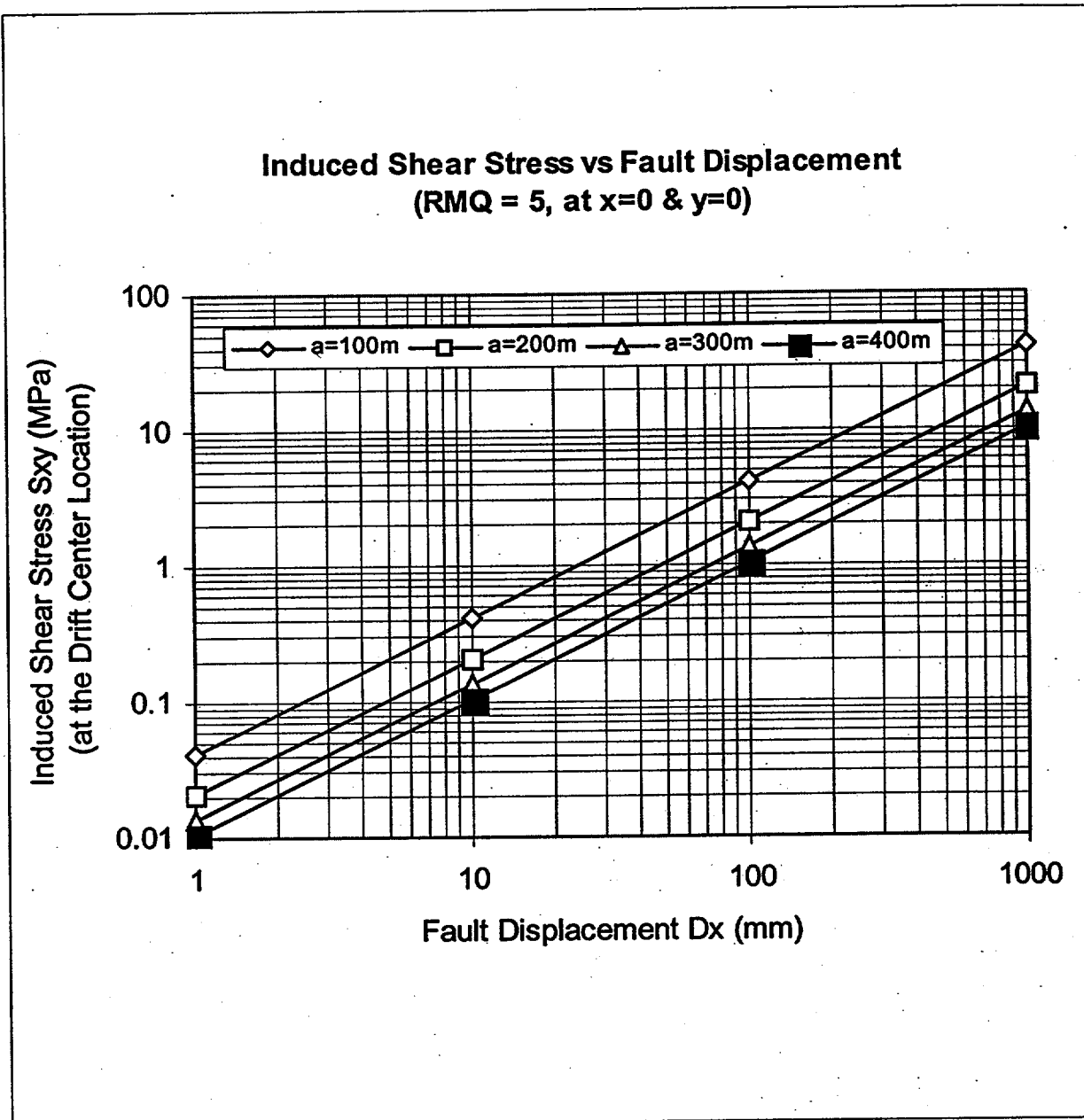


Figure 18. Induced Shear Stress at the Location of an Emplacement Drift vs. Fault Displacement: RMQ = 5, Distance between the Drift and Fault = 0 m.

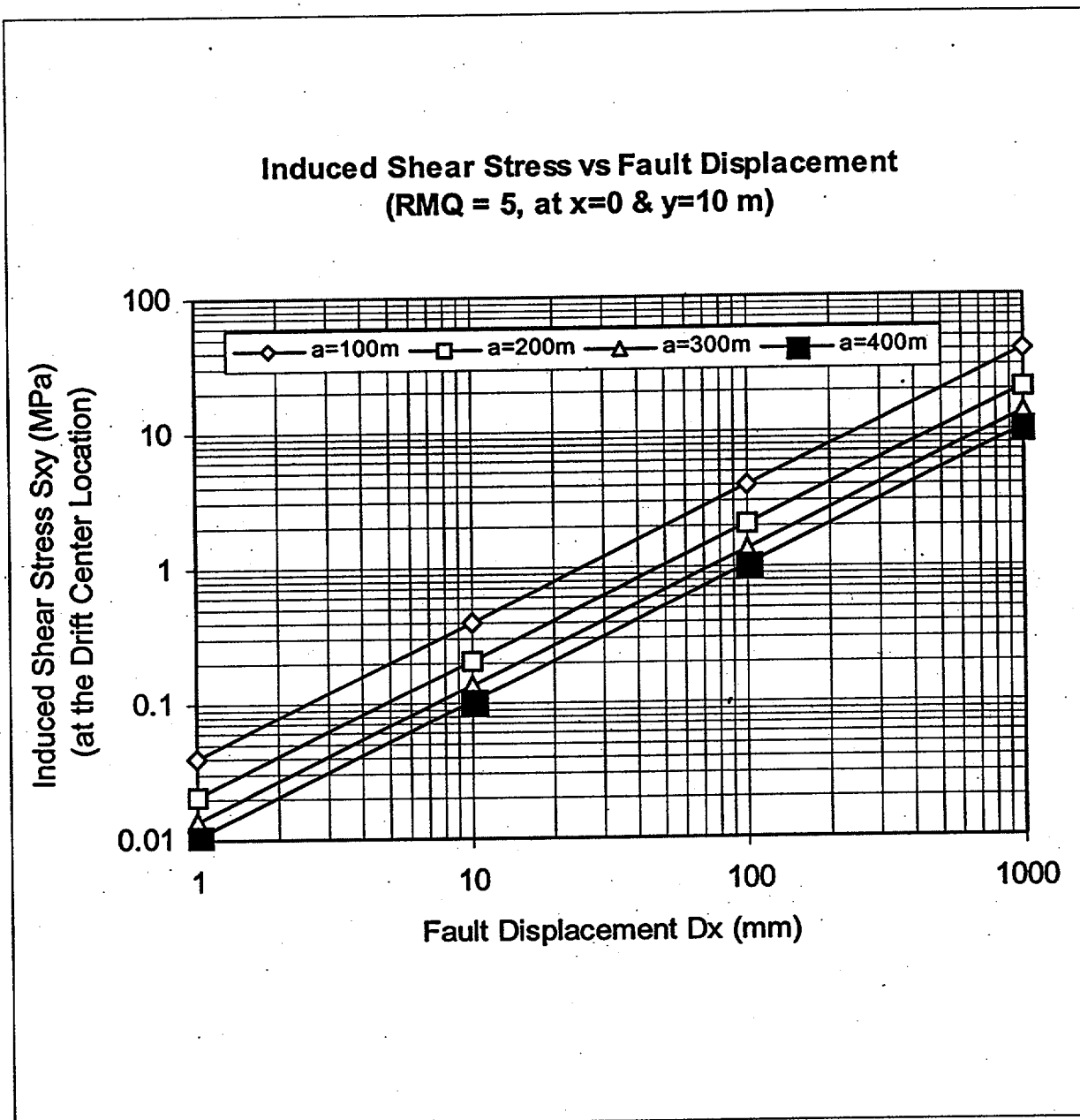


Figure 19. Induced Shear Stress at the Location of an Emplacement Drift vs. Fault Displacement: RMQ = 5, Distance between the Drift and Fault = 10 m.

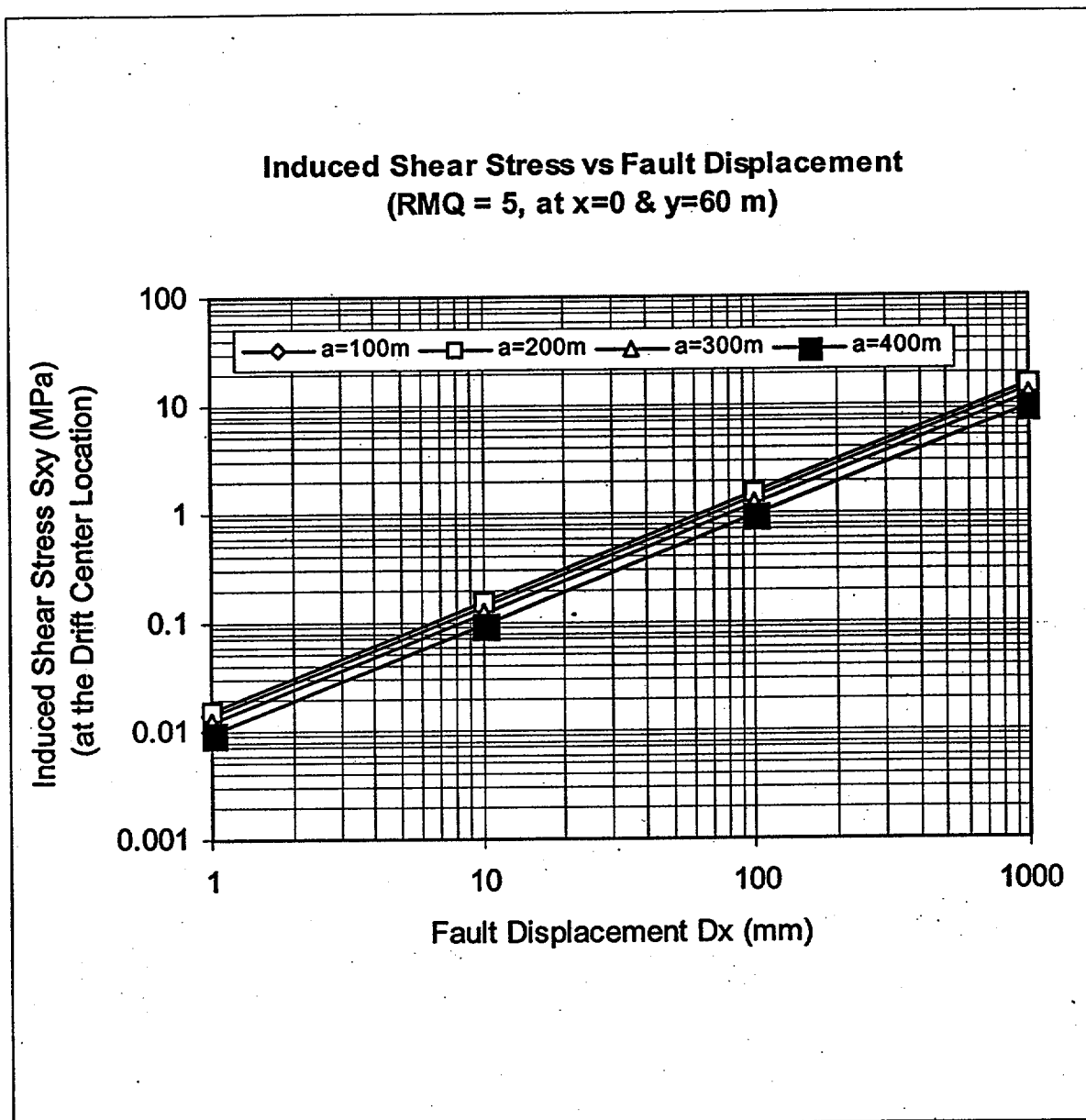


Figure 20. The Induced Shear Stress at the Location of an Emplacement Drift vs. Fault Displacement: RMQ = 5, Distance between the Drift and Fault = 60 m.

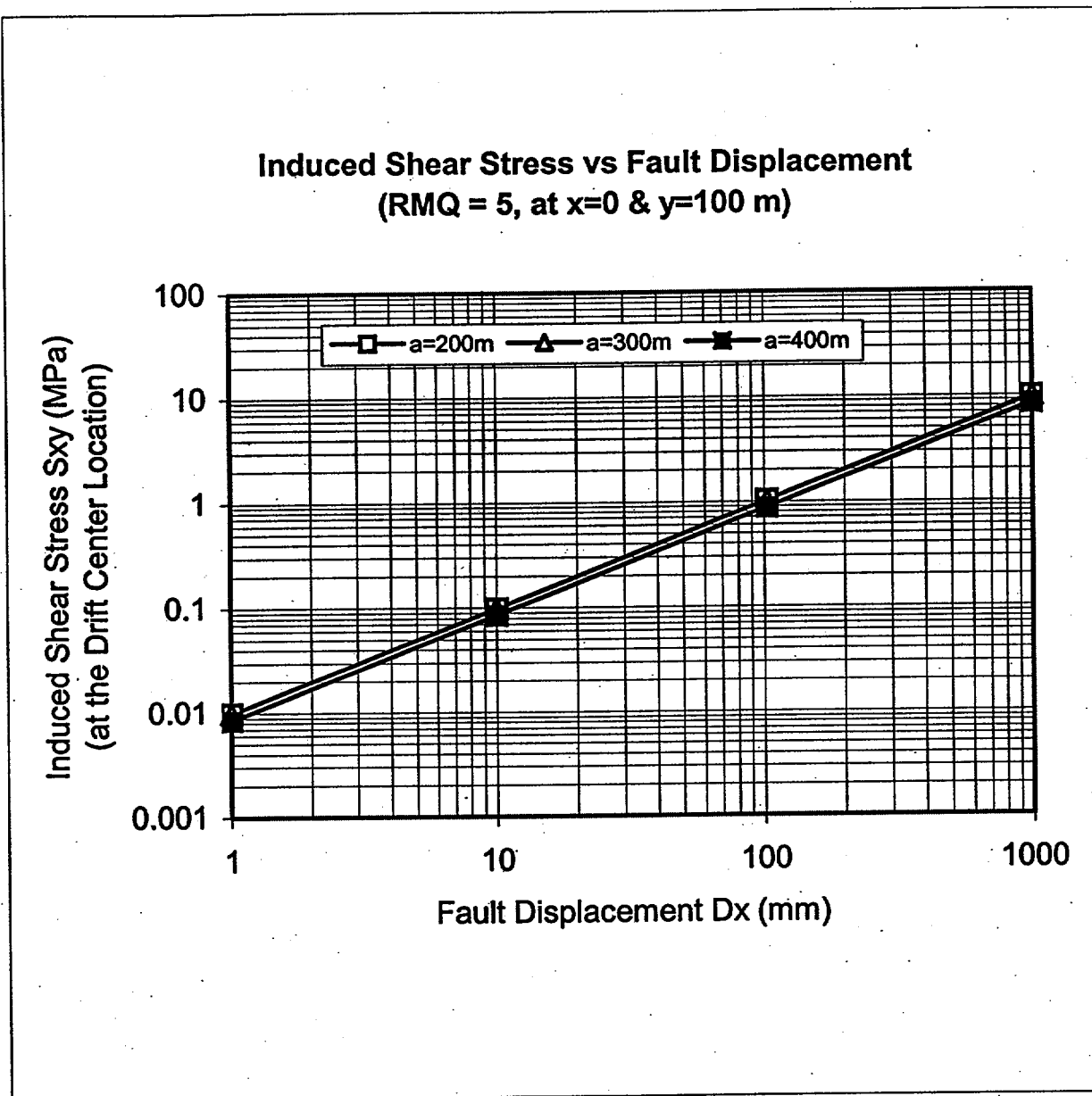


Figure 21. Induced Shear Stress at the Location of an Emplacement Drift vs. Fault Displacement: RMQ = 5, Distance between the Drift and Fault = 100 m.

6.4.2. Strike-Slip Faulting Scenario

Use of expression (18) requires an estimate of $\sigma_{xz,0}$. This stress component is the shear stress existing prior to the occurrence of fault displacement, and its shearing direction is parallel to the strike of the fault. A crude estimate of $\sigma_{xz,0}$ at the repository host horizon is to take the half of the maximum difference between the two horizontal in situ stresses, i.e.,

$$\begin{aligned}\sigma_{xz,0} &= 0.5*(\sigma_{hmax} - \sigma_{hmin}) = 0.5(1.0 \sigma_v - 0.3 \sigma_v) \\ &= 0.5*(1.0 - 0.3)*10 \text{ MPa} = 3.5 \text{ MPa. (See Section 5.7)}\end{aligned}$$

By substituting $\sigma_{xz,0} = 3.5 \text{ MPa}$ into expression (18), the induced shear stress (σ_{xz}) becomes a function of a and y , i.e., $\sigma_{xz} = 3.5y/(y^2 - a^2)^{1/2}$. For example, consider $a = 300 \text{ m}$ and $y = 310 \text{ m}$, corresponding to a scenario where an emplacement drift is located 10 m ($= 310 - 300$) directly underneath a 300 m deep strike-slip fault, then $\sigma_{xz} = 3.5 \times 310 / (310^2 - 300^2)^{1/2} = 13.89 \text{ MPa}$ or $\sigma_{xz} / \sigma_{xz,0} = 3.97$. Figure 22 shows the resultant normalized shear stress vs. the vertical distance from the strike-slip fault. Assumptions 5.8 and 5.9 are used in generating Figure 22. As expected, the more extensive (i.e., larger length along the dip) a strike-slip fault is, the more pronounced the fault effects become. Since there are no material properties entering expression (18), the shear stress induced in the vicinity of a strike-slip fault is independent of the rock mass conditions. As the distance from the fault increases, the shear stress decreases towards the initial value prior to the fault eruption.

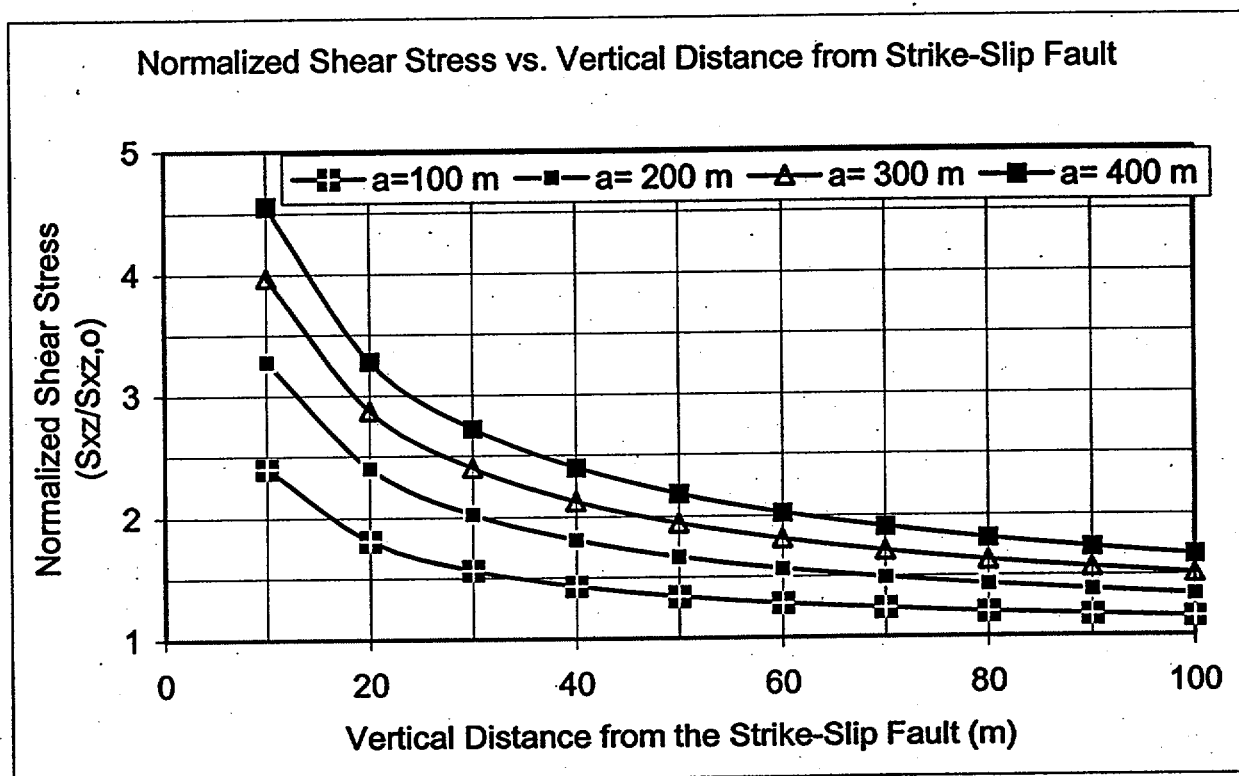


Figure 22. Effect of a Strike-Slip Fault on Emplacement Drift Located below the Fault

6.5. DISCUSSION

6.5.1. Fault Displacement Effects on Drifts

By neglecting the ground support system, the effects of fault displacement on emplacement drifts manifest themselves in terms of impedance to the operational clearance envelope and disturbance to drift stability. The former relates to the induced rock movement at the emplacement drift location while the latter depends on the status of the resultant stresses caused by excavation, thermal loading and fault activity.

The degree of impedance to the operational clearance envelope depends on both the magnitude of fault displacement and the location of the fault with respect to the emplacement drift location. The maximum impedance occurs when a steeply-dipping fault intersects an emplacement drift at the crown and invert areas. Such a scenario corresponds to the $x = 0$ and $y = 0$ case shown in Figures 6 and 7. In this case, the maximum offset of the emplacement drift is equal to the fault displacement. Obviously, the fault displacement of a few millimeters causes negligible impedance no matter where the fault is located. As expected, Figures 6 and 7 show that the rock movement induced by fault displacement at an emplacement drift location decreases slowly but surely as the distance between the drift and fault becomes greater. For a fault displacement of about 300 mm, which closely corresponds to the maximum mean fault displacement (320 mm) tabulated in Table 1 for the Solitario Fault, a drift 60 m away from the fault is predicted to experience about 100 to 150 mm rock movement, depending on the extent of the fault along the dip.

Stresses induced at the emplacement drift location depend on the rock mass quality category and are linearly proportional to the shear modulus value of the rock mass. Therefore, for a given fault displacement, the induced stresses at an emplacement drift location for $RMQ = 5$ are 2.75 times ($G_{RMQ=5}/G_{RMQ=1} = 2.75$) those for $RMQ = 1$. The induced normal stress component (σ_{xx}) is much lower than the shear stress (σ_{xy}), as can be seen by a comparison between Figures 13 and 21. Figure 13 corresponds to a location at $x = 50$ and $y = 100$ m while Figure 21 corresponds to a location at $x = 0$ and $y = 100$ m. Since the induced normal stress at the location shown in Figure 21 is zero, a nearby point is used for comparison. Subsequent discussions focus on the induced shear stress. Table 5 summarizes the results in accordance with the fault displacement values presented in Tables 1 and 2.

Table 5 shows that a fault displacement of 1 mm induces a negligible amount (less than 0.1 MPa) of stress disturbance at the emplacement drift location. On the other hand, a fault displacement comparable to those at Bow Ridge and Solitario Canyon faults can induce noticeable shear stresses at the emplacement drift location if the fault is close to the drift. Fault displacement induces much higher shear stress in the $RMQ = 5$ rock mass category than in the $RMQ = 1$ rock mass category. If the induced shear stress is treated as pure shear, the principal stresses ($\sigma_1 = -\sigma_3 = \sigma_{xy}$) are obtained. By superimposing these induced stresses onto the existing stresses surrounding an emplacement drift, impact on drift stability can be evaluated by using a yield criterion. No determination of the existing stresses, except for in situ stresses, is given in this analysis. Considering that the vertical in situ stress at the emplacement drift level is 10 MPa, any induced stress of, say, more than 1 MPa should be considered significant. In this respect, a fault displacement comparable with those at Bow Ridge fault and Solitario Canyon fault would result

in a significant disturbance if such a fault is close to the emplacement drift. At 60 m from the fault, the induced stress is reduced by more than 60%, supporting criterion 4.2.1.

Results based on the strike-slip fault calculations, see Figure 22, show a rapid initial decrease in induced shear stress with increasing distance from the fault. The results support the 60 m offset distance criterion.

Table 5. Induced Shear Stress at the Emplacement Drift Location

Fault Displacement (mm)	Maximum Induced Shear Stress (MPa)					
	y = 0		y = 60 m		y = 100 m	
	RMQ=1	RMQ=5	RMQ=1	RMQ=5	RMQ=1	RMQ=5
1 mm (corresponding to fault displacement away from principal faults)	0.015 (Fig. 14, a=100 m)	0.04 (Fig. 18, a=100m)	0.005 (Fig. 16, a=100 m)	0.014 (Fig. 20, a=100 m)	0.0036 (Fig. 17, a=200 m)	0.01 (Fig. 21, a=200m)
100 mm (conservatively approximating the fault displacement of 7.8 cm at Bow Ridge fault)	1.5 (Fig. 14, a=100 m)	4 (Fig. 18, a=100m)	0.5 (Fig. 16, a=100 m)	1.4 (Fig. 20, a=100 m)	0.36 (Fig. 17, a=200 m)	1 (Fig. 21, a=200 m)
300 mm (approximately corresponding to the fault displacement of 32 cm at Solitario Canyon fault)	4.5 (Fig. 14, a=100 m)	12 (Fig. 18, a=100m)	1.5 (Fig. 16, a=100 m)	4.3 (Fig. 20, a=100 m)	1.08 (Fig. 17, a=200 m)	3 (Fig. 21, a=200 m)

6.5.2. Fault Displacement Effects on Drip Shields

A drip shield is designed to shield the waste package from moisture and to divert water flow to the invert, as illustrated in Figure 23. At issue is whether a fault displacement will disrupt the function of a drip shield. Analytical results of fault displacement effects on emplacement drifts discussed earlier can be used to qualitatively address the issue.

Figure 24 helps put the issue in perspective. Since there is a gap between the backfill and drift wall, particularly above the spring line, it is unlikely that a fault displacement will result in a load transfer from the rock to backfill or drip shield. In other words, the gap must be closed before the fault displacement-induced rock movement can load the backfill, which in turn loads the drip shield. However, any induced shear stress present in the invert may impact the drip shield, depending on the connection between the drip shield and invert.

For the sake of conservative argument, consider the scenario where backfill is full, fully contacting the drift wall. The stresses induced by fault displacement in backfill will be much lower than those induced in the rock because of high porosity and low modulus. As expression (10) indicates, the induced shear stress is proportional to the shear modulus value. Since backfill

materials will be non-cementitious, it is quite likely that the shear modulus of the backfill will be at least an order of magnitude less than that of the rock. Consequently, the induced shear stress in backfill, if any, would be at least an order of magnitude less than those tabulated in Table 5 for the rock, rendering the building up of the induced stress in backfill negligible. A negligible induced load on the backfill leads to a negligible load on the drip shield that acts to contain the backfill.

It must be pointed out that loads other than shear may be induced in a drip shield if a fault intersects an emplacement drift. These loads may include bending and twisting, but are not considered in this analysis. For instance, a strike-slip fault that intersects an emplacement drift at an acute angle (particularly parallel or sub-parallel to the drift axis) may shear the invert such that rotation and distortion may occur in a drip shield. Sophisticated numerical methods are required in order to quantify these loads and examine their effects on a drip shield. However, since the emplacement drift area lies between the Solitario Canyon and Ghost Dance faults, the probability of having a new fault intersect the invert of an emplacement drift is extremely low, as can be seen from PSHA results at demonstration points 7c and 8c (CRWMS M&O 1998d, Figures 8-10 and 8-13). These two demonstration points are located within the emplacement drift footprint. Therefore, the impact from such an unlikely scenario is not considered to be consequential either during preclosure or postclosure.

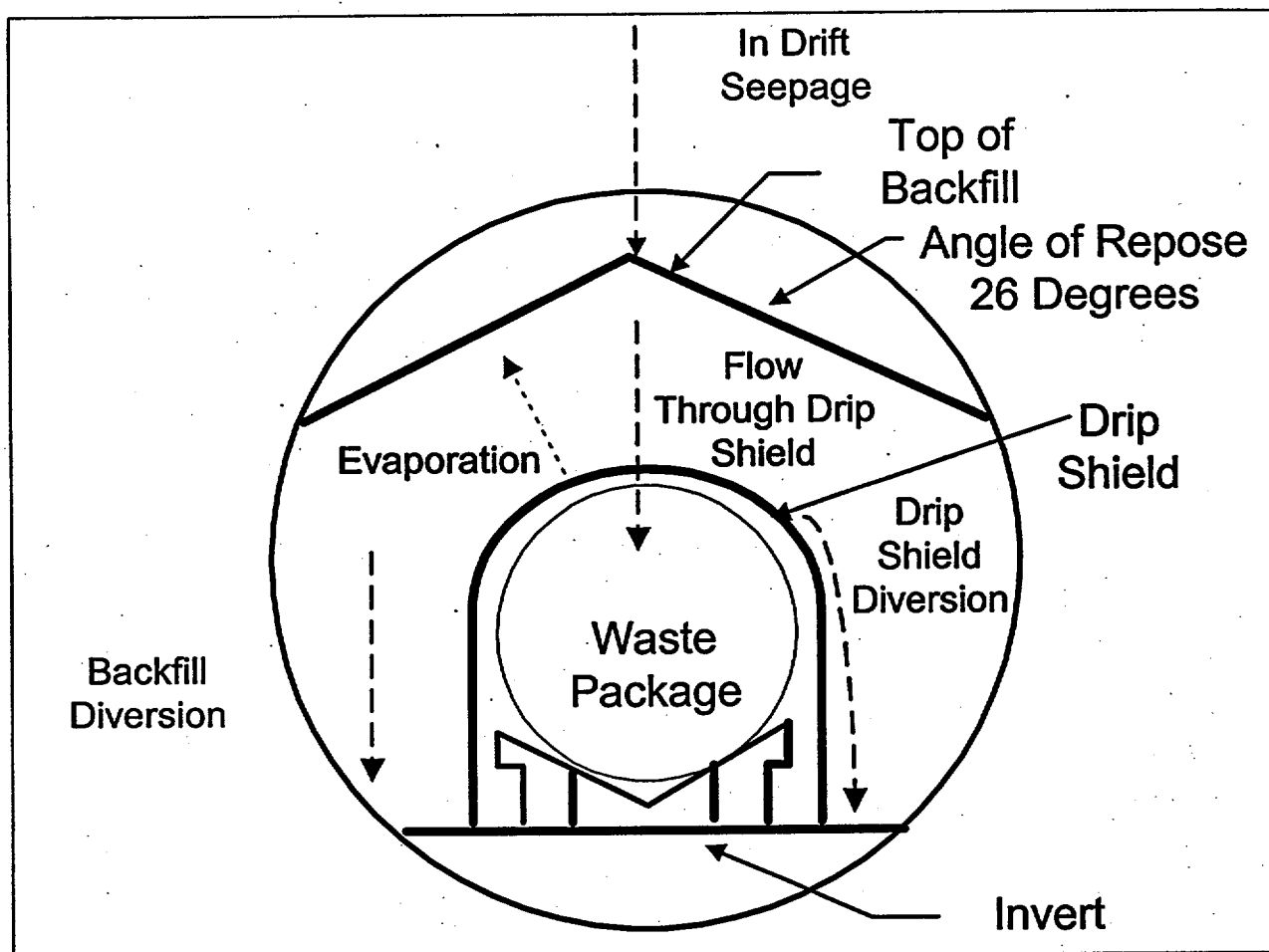


Figure 23. A Schematic of Waste Package, Drip Shield and Backfill.

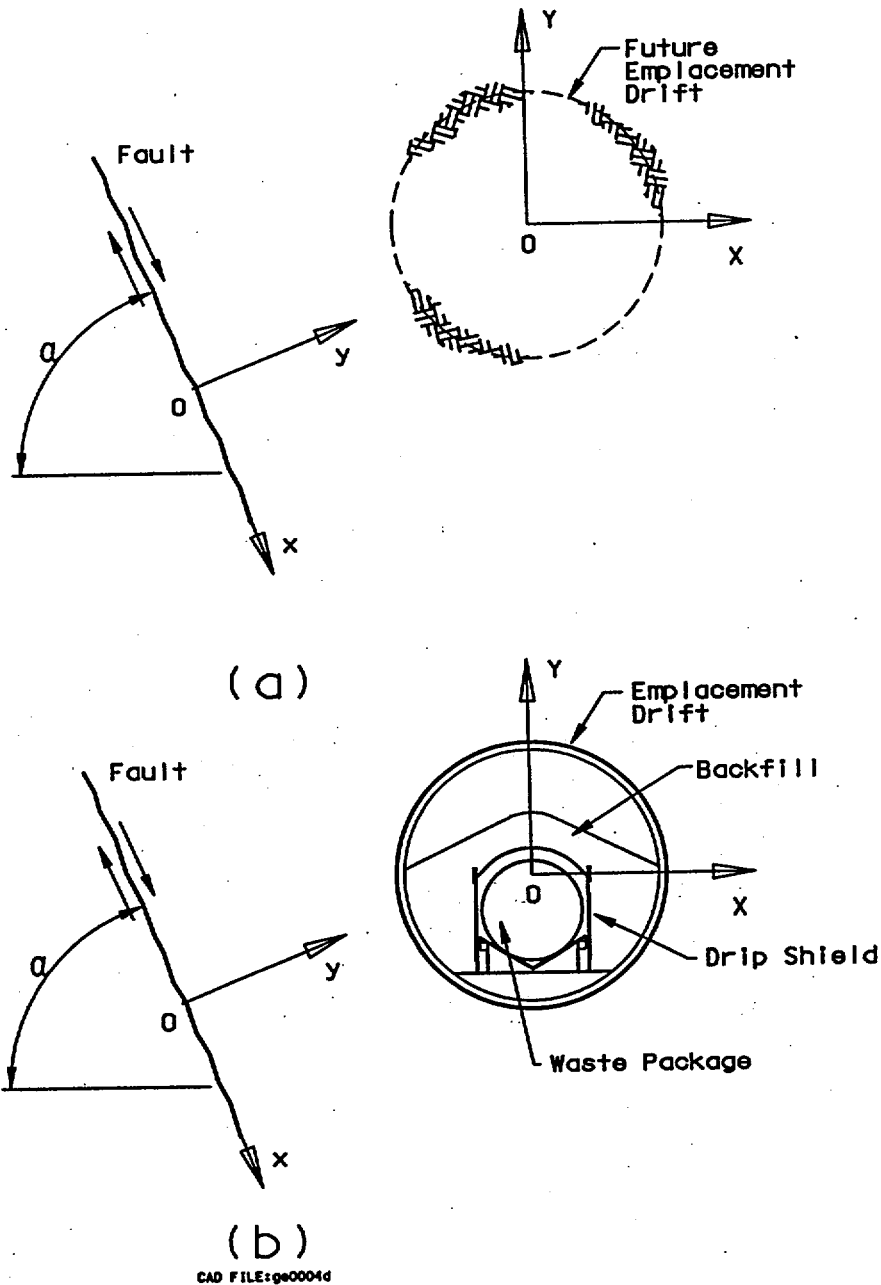


Figure 24. A Schematic Diagram for Estimating Fault Displacement Effects on Drip Shield: (a) Drift Excavation for Which Fault Displacement Effects Are Evaluated; (b) After Drip Shield Installation for Which Fault Displacement Effects Are to Be Estimated

6.5.3. Fault Displacement Effects on Waste Packages

The potential effects of fault displacement on waste packages are considered without the presence of drip shields. Whether backfill is used or not, fault displacement effects on waste packages are similar in principle to fault displacement effects on drip shields. Without backfill, even the maximum fault displacement associated with principal faults should not have any effects on waste packages as long as these faults do not cut through the drift invert. If a fault intersects the drift invert, the shearing action on the invert may have an adverse impact on the waste package, depending on the type of connection between the waste package and invert. If a relatively rigid connection is present, the fault displacement occurring at the invert will transfer a considerable load to the waste package. On the other hand, a relatively flexible connection will absorb most of the fault displacement without subjecting the waste package to significant fault displacement-induced loads.

With backfill, it is unlikely for the fault displacement to cause the drift wall to move so much that the backfill is compressed and a considerable amount of compression load is transferred to waste packages. Therefore, the potential for fault displacement effects on waste packages may exist only when a fault, either normal or strike-slip type, intersects the drift invert where waste packages sit. A fault displacement of tens of centimeter could cause rotation, bending, and tilting of a waste package. In that case, external loads would be exerted on the waste package. These loading scenarios are not covered in this analysis. As is stated in Section 6.5.2, the likelihood of having a new fault intersect the invert of an emplacement drift is extremely low, the impact from such an unlikely scenario is not considered to be consequential either during preclosure or postclosure.

7. CONCLUSIONS

Based on closed-form solutions of simplified diagrams of normal and strike-slip faults, effects of fault displacement on emplacement drift, drip shield and waste package have been assessed. These effects are described in terms of displacement and stress induced by fault displacement. Discussions have mainly focused on the preclosure fault displacement. No credit is taken of ground support systems. The analysis has considered a constant fault displacement ranging from 0.1 to 100 cm. The largest mean preclosure fault displacement is 32 cm at the Solitario Canyon fault. In this respect, a 100 cm fault displacement considered in this analysis extends into the postclosure period. The following conclusions are drawn:

- Depending on the location of a fault relative to the emplacement drift location, fault displacement could induce detectable stresses and rock movement at the emplacement drift vicinity. Considering two extreme rock mass quality categories, that is, $RMQ = 1$ and $RMQ = 5$, a fault displacement comparable to those at Bow Ridge and Solitario Canyon would induce a shear stress of 1.4 to 4.3 MPa at an emplacement drift location if the fault is located 60 m away. The induced shear stress decreases to 1 to 3 MPa if the fault is 100 m away. Higher stress is associated with higher RMQ category. These induced stress levels are not considered to be detrimental to drift stability.
- Effects of fault displacement on drip shield were evaluated by treating fault displacement effects on an unexcavated emplacement drift location as a bounding scenario. Backfill present in an emplacement drift acts as soft inclusion in a solid and will draw less stress than its surrounding stiff medium. Partly because of backfill's high compressibility due to its voids and partly because of the presence of gap between backfill and drift wall particularly above the spring line, it was estimated that stresses induced by fault displacement in backfill, if any, would be negligibly small unless a fault displacement over a meter in magnitude occurs. A negligible induced load in backfill renders any induced load in a drip shield negligible. Consequently, effects of fault displacement on drip shield are of no concern as long as emplacement drifts are not directly intersected by faults. As currently planned, major faults will not directly intersect emplacement drifts.
- Similar to drip shield, waste packages are unlikely to be subject to loading effects induced by fault displacement regardless of the presence of backfill or not.
- Evaluation results presented in this analysis support the fault avoidance design criterion. For faults with fault displacements comparable to those at Bow Ridge and Solitario Canyon, fault avoidance is especially prudent. These faults are shown to induce considerable stress and rock movement when they are close to emplacement drifts.

It must be pointed out that loads other than normal and shear stresses may be induced in a drip shield or waste package if a fault intersects an emplacement drift. These loads may include bending and twisting when the drift invert is intersected by a fault, subjecting the drip shield and waste package to rotation, distortion or tilting. Sophisticated numerical models are required in order to quantify these loads and examine their effects on drip shields and waste packages. However, the probability of having a new fault intersect the invert of an emplacement drift is

extremely low, as can be seen from PSHA results at demonstration points 7c and 8c (CRWMS M&O 1998d, Figures 8-10 and 8-13). These two demonstration points are located within the emplacement drift footprint. Therefore, the impact from such an unlikely scenario is not considered to be consequential either during preclosure or postclosure.

It must be pointed out that the mean fault displacement associated with the annual exceedance probability of 10^{-5} is used as yardstick in evaluating fault displacement effects in terms of the induced stress and displacement at an emplacement drift location. Should a lower annual exceedance probability be considered for the postclosure period, the corresponding mean fault displacement value would increase. It is uncertain whether or not the results calculated at a 100 cm fault displacement are adequate enough to cover lower annual exceedance probability scenarios. Although this analysis generally shows that fault displacement effects in terms of the induced stress and displacement decrease as the fault rupture length along the fault increases, caution must be taken in attempting to extrapolate the results for a much longer fault length in the dip direction, say, $a = 10,000$ m. In general, any significant deviation from the assumptions and input parameters listed in this analysis calls for a re-evaluation of the results presented in this analysis.

There are no new TBVs or TBDs generated in this analysis. Existing TBVs are mentioned in Sections 2 and 4.2. Those TBVs have no impact on the results of this analysis.

8. REFERENCES

- Crouch, S.L. and Starfield, A.M. 1983. *Boundary Element Methods in Solid Mechanics: with Applications in Rock Mechanics and Geological Engineering*. Boston, Massachusetts: Allen & Unwin. TIC #4370.
- CRWMS M&O 1998a. *Subsurface Facility System Description Document*. BCA000000-01717-1705-00014 REV 00. Las Vegas, Nevada: CRWMS M&O. ACC: MOL.19980826.0161.
- CRWMS M&O 1998b. *Ground Control System Description Document*. BCA000000-01717-1705-00011 REV 00. Las Vegas, Nevada: CRWMS M&O. ACC: MOL.19980825.0286.
- CRWMS M&O 1998c. *Repository Ground Support Analysis for Viability Assessment*. BCAA00000-01717-0200-00004 REV 01. Las Vegas, Nevada: CRWMS M&O. ACC: MOL.19980512.0714.
- CRWMS M&O 1998d. *Probabilistic Seismic Hazard Analyses for Fault Displacement and Vibratory Ground Motion at Yucca Mountain, Nevada*. I. G. Wong and J. C. Stepp, Report Coordinators. Milestone Report SP32IM3 Prepared for the U.S. Geological Survey. Oakland, California: CRWMS M&O. ACC: MOL.19981207.0393.
- CRWMS M&O 1999a. *Effects of Fault Displacement on Emplacement Drifts*. Development Plan (DP) Checklist and Cover Sheet. TDP-EBS-GE-000002 REV 01. Las Vegas, Nevada: CRWMS M&O. ACC: MOL.19991220.0376.
- CRWMS M&O 1999b. *Activity Evaluation: Ground Control – 99 (FY 99WP #12012383MD) All RPT1000 Series*. Las Vegas, Nevada: CRWMS M&O. ACC: MOL.19990727.0239.
- CRWMS M&O 1999c. *Classification of the MGR Subsurface Facility System*. ANL-SFS-SE-000001 REV 00. Las Vegas, Nevada: CRWMS M&O. ACC: MOL.19990928.0214.
- CRWMS M&O 1999d. *Classification of the MGR Ground Control System*. ANL-GCS-SE-000001 REV 00. Las Vegas, Nevada: CRWMS M&O. ACC: MOL.19990928.0217.
- CRWMS M&O 1999e. *TBV-332/TBD-325 Resolution Analysis: Geotechnical Rock Properties*. B00000000-01717-5705-00134 REV 00. Las Vegas, Nevada: CRWMS M&O. ACC: MOL.19991005.0235.
- U.S. Department of Energy (DOE)/Office of Civilian Radioactive Waste Management (OCRWM) 1997. *Preclosure Seismic Design Methodology for a Geologic Repository at Yucca Mountain*. Topical Report YMP/TR-003-NP, Revision 2. Las Vegas, Nevada: DOE/OCRWM. ACC: MOL.19971009.0412.
- DOE/OCRWM 1998a. *Quality Assurance Requirements and Description for the Civilian Radioactive Waste Management Program*. DOE/RW/0333P, REV 08. Washington, D.C.: DOE/OCRWM. ACC: MOL.19980601.0022.

DOE/OCRWM 1998b. *Q-List*. YMF/90-55Q, Revision 5. Las Vegas, Nevada: DOE/OCRWM. ACC: MOL.19980513.0132.

Duncan, J.M. and Lefebvre, G. 1973. "Earth Pressures on Structures Due to Fault Movement". *Journal of the Soil Mechanics and Foundations Division*, 105(SM12), 1153-1163. New York, New York: American Society of Civil Engineers (ASCE). TIC: 226234.

Kennedy, R.P., Chow, A.W., and Williamson, R.A. 1977. "Fault Movement Effects on Buried Oil Pipeline". *Transportation Engineering Journal*, 103(TE5), 617-633. New York, New York: American Society of Civil Engineers (ASCE). TIC: 226245.

Kennedy, R.P., Darrow, A.C., and Short, S.A. 1979. "Seismic Design of Oil Pipeline System". *Journal of the Technical Councils of ASCE*, 103(TC1), 119-134. New York, New York: American Society of Civil Engineers (ASCE). TIC: 246580.

Nuclear Regulatory Commission (NRC) 1992. *Staff Technical Position on Investigations to Identify Fault Displacement Hazards and Seismic Hazards at a Geologic Repository*. K.I. McConnell, M.E. Blackford, and A.K. Ibrahim (Authors). NUREG-1451. Washington, D. C.: NRC. TIC: 204829.

NRC 1994. *Staff Technical Position on Consideration of Fault Displacement Hazards in Geologic Repository Design*. K.I. McConnell and M.P. Lee (Authors). NUREG-1494. Washington, D. C.: NRC. TIC: 212360.

Turcotte, D.L. and Schubert, G. 1982. *Geodynamics Applications of Continuum Physics to Geological Problems*. New York, New York: John Wiley & Sons. TIC: 235924.

9. ATTACHMENTS

None.